(4)

AFGL-TR-88-0130 SSS-R-88-9595

HIGH FREQUENCY SEISMIC SOURCE CHARACTERISTICS OF CAVITY DECOUPLED UNDERGROUND NUCLEAR EXPLOSIONS

J. R. MURPHY
J. L. STEVENS
N. RIMER

S-CUBED
A DIVISION OF MAXWELL LABORATORIES, INC.
P. O. BOX 1620
LA JOLLA, CALIFORNIA 92038-1620

MAY 1988

SCIENTIFIC REPORT NO. 1

AIR FORCE GEOPHYSICS LABORATORY
AIR FORCE SYSTEMS COMMAND
UNITED STATES AIR FORCE
HANSCOM AIR FORCE BASE,
MASSACHUSETTS 01731-5000

DISCLAIMER NOTICE

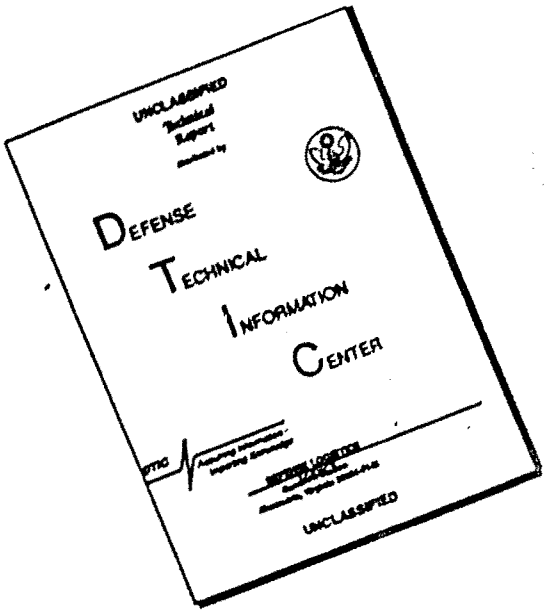

THIS DOCUMENT IS BEST QUALITY AVAILABLE. THE COPY FURNISHED TO DTIC CONTAINED A SIGNIFICANT NUMBER OF PAGES WHICH DO NOT REPRODUCE LEGIBLY.

UNCLASSIFIED
SECURITY CLASSIFICATION OF THIS PAGE

REPORT DOCUMENTATION PAGE

1a. REPORT SECURITY CLASSIFICATION UNCLASSIFIED	1b. RESTRICTIVE MARKINGS
2a. SECURITY CLASSIFICATION AUTHORITY	3. DISTRIBUTION/AVAILABILITY OF REPORT Approved for public release; distribution unlimited.
2b. DECLASSIFICATION/DOWNGRADING SCHEDULE	
4. PERFORMING ORGANIZATION REPORT NUMBER(S) SSS-R-88-9595	5. MONITORING ORGANIZATION REPORT NUMBER(S) AFGL-TR-88-0130
6a. NAME OF PERFORMING ORGANIZATION S-Cubed Div. of Maxwell Labs. — 6b. OFFICE SYMBOL (If applicable)	7a. NAME OF MONITORING ORGANIZATION Air Force Geophysics Laboratory/LWH
6c. ADDRESS (City, State, and ZIP Code) P. O. Box 1620 La Jolla, California 92038-1620	7b. ADDRESS (City, State, and ZIP Code) Hanscom Air Force Base Massachusetts 01731
8a. NAME OF FUNDING/SPONSORING ORGANIZATION Defense Advanced Research Projects Agency — 8b. OFFICE SYMBOL (If applicable) DSO/GSD	9. PROCUREMENT INSTRUMENT IDENTIFICATION NUMBER F19628-87 C-0093
8c. ADDRESS (City, State, and ZIP Code) 1400 Wilson Boulevard Arlington, Virginia 22209	10. SOURCE OF FUNDING NUMBERS PROGRAM ELEMENT NO. 62714E — PROJECT NO. 7A10 — TASK NO. DA — WORK UNIT ACCESSION NO. DB
11. TITLE (Include Security Classification) HIGH FREQUENCY SEISMIC SOURCE CHARACTERISTICS OF CAVITY DECOUPLED UNDERGROUND NUCLEAR EXPLOSIONS (U)	
12. PERSONAL AUTHOR(S) J. R. Murphy, J. L. Stevens and N. Rimer	
13a. TYPE OF REPORT Scientific No. 1 — 13b. TIME COVERED FROM 870322 TO 880322 — 14. DATE OF REPORT (Year, Month, Day) May, 1988 — 15. PAGE COUNT 76	
16. SUPPLEMENTARY NOTATION	
17. COSATI CODES FIELD / GROUP / SUB-GROUP	18. SUBJECT TERMS (Continue on reverse if necessary and identify by block number) Cavity Decoupling/ High Frequency / STERLING Seismic Source / Nonlinear Simulation Nuclear Explosion / Tuff / Salt / MILL YARD

19. ABSTRACT (Continue on reverse if necessary and identify by block number)

The objectives of the research summarized in this report have been to conduct a more rigorous theoretical investigation of the high frequency characteristics of the seismic sources corresponding to cavity decoupled nuclear explosions and to assess the implications of these investigations with regard to the detection and discrimination of small decoupled explosions. This study has been carried out using a combination of deterministic simulations and analyses of empirical data recorded from selected cavity decoupled explosions.

With regard to the deterministic simulations, a series of nonlinear finite difference calculations have been performed to simulate cavity decoupled explosions in unsaturated tuff and salt emplacement media. These
(continued on reverse)

20. DISTRIBUTION/AVAILABILITY OF ABSTRACT ☐ UNCLASSIFIED/UNLIMITED ☒ SAME AS RPT. ☐ DTIC USERS	21. ABSTRACT SECURITY CLASSIFICATION UNCLASSIFIED
22a. NAME OF RESPONSIBLE INDIVIDUAL James Lewkowicz	22b. TELEPHONE (Include Area Code) 617/377-3028 — 22c. OFFICE SYMBOL LWH

DD FORM 1473, 84 MAR — 83 APR edition may be used until exhausted. All other editions are obsolete.

SECURITY CLASSIFICATION OF THIS PAGE
UNCLASSIFIED

19. (Continued)

simulations have confirmed the fact that the simple step pressure approximation is not valid at high frequencies and that the initial pressure spike on the cavity wall can induce significant nonlinear response. In particular, all the simulations conducted to date indicate enhanced seismic coupling at high frequency relative to that predicted using the classical step pressure approximation.

Preliminary analyses of high frequency seismic data recorded from the STERLING decoupled explosion in salt and the MILL YARD decoupled explosion in unsaturated tuff have provided evidence that the high frequency source components associated with the complex cavity pressure loadings do effectively couple into the seismic regime, in agreement with the predictions of the nonlinear finite difference simulations. However, the observed complexity of the propagation effects at high frequency raises questions as to whether such source characteristics can be reliably recovered from the recorded seismic data and used for identification purposes.

TABLE OF CONTENTS

LIST OF ILLUSTRATIONS

LIST OF ILLUSTRATIONS (Continued)

LIST OF ILLUSTRATIONS (Continued)

I. INTRODUCTION

Cavity decoupled underground nuclear explosions in the yield range from 1 to 10 kt can be expected to generate seismic signals corresponding to m_b values in the 2.0 to 3.0 range and, consequently, such events pose a severe test for a seismic monitoring network. In particular, even assuming the existence of an internal network capable of detecting such events, it is not yet clear how they could be differentiated from the background of many small earthquakes and routine chemical explosions of comparable size which can be expected to be detected by the network. Evernden et al. (1986) and others have suggested that it may be possible to resolve this discrimination problem using high frequency (> 20 Hz) seismic data. However, these arguments are speculative to the extent that little is currently known about the high frequency source characteristics of such events, particularly for cavity decoupled explosions. The objectives of the research summarized in this report have been to conduct a more rigorous theoretical investigation of the high frequency characteristics of decoupled seismic sources and to assess the implications of these investigations with regard to the detection and discrimination of small decoupled explosions. This is being accomplished through a combination of detailed deterministic simulations and analyses of empirical data recorded from selected cavity decoupled explosions.

The organization of this report may be briefly summarized as follows. A review of decoupling phenomenology is presented in Section II, with specific emphasis on those aspects of the problem affecting high frequency coupling effectiveness. This is followed in Section III by a description of the results of a series of detailed, nonlinear finite difference calculations which have been carried out to simulate the seismic source functions corresponding to coupled and

decoupled explosions in unsaturated tuff and salt emplacement media. Results of preliminary analyses of high frequency seismic data recorded from the STERLING decoupled explosion in salt and the MILL YARD decoupled explosion in unsaturated tuff are presented in Section IV. This is followed in Section V by a summary and a statement of preliminary conclusions regarding high frequency seismic monitoring of small decoupled explosions.

II. REVIEW OF DECOUPLING PHENOMENOLOGY

The concept that it might be possible to significantly reduce the seismic signal radiated by an underground nuclear explosion by detonating the device in a cavity (i.e., cavity decoupling) was first proposed publicly by A. L. Latter at the 1959 Nuclear Test Ban Conference in Geneva (Latter, 1959). However, despite the fact that nearly 30 years have now elapsed since its introduction, a number of major issues of importance with respect to seismic monitoring still remain unresolved. This is particularly true with regard to the potential utility of high frequency seismic data of the type which might eventually be collected by regional, in-country monitoring stations. Before proceeding on to a detailed theoretical consideration of these issues, it is appropriate to first review some of the general principles governing the seismic source characteristics of coupled and decoupled underground nuclear explosions.

Surrounding every fully coupled underground explosion is a region in which the material response is nonlinear. This corresponds to the regime where the shock pressure is high enough to cause vaporization, crushing and cracking of the medium. As the range from the detonation point increases, however, the shock pressure decays to a level (P_{el}) at which the response is linear and it is the forcing function acting at this radius which defines the characteristics of the radiated seismic waves which are used for detection and discrimination purposes. This radius is commonly called the elastic radius and denoted as r_{el}. Consider the case in which the pressure function acting at r_{el} is a simple step in pressure, $P_{el}\ H(t)$. Then, it can be shown (Mueller and Murphy, 1971) that the amplitude of the seismic source function, $S(\omega)$, in the low frequency limit is given by

$$\lim_{\omega \to 0} \quad |S(\omega)| \quad \sim \quad P_{el} \quad r_{el}^{3} \tag{1}$$

Now, if P_{el} is proportional to the overburden pressure, ρgh, then it follows from (1) that, at a fixed depth h, the low frequency coupling efficiency will depend only on r_{el}. But, to a first approximation, the peak shock pressure decreases with distance r as r^{-n} where n is the medium-dependent attenuation rate. Thus, r_{el} decreases as n increases, and the reason cavity decoupling works is that for strong shocks in air n = 3, while in rock $n \approx 2$ (Brode, 1968; Rodean, 1971). That is, an explosion is said to be fully decoupled if it is detonated in a cavity which is large enough that the surrounding medium undergoes no nonlinear deformation. It follows from the above discussion that the radius of the cavity required to fully decouple an explosion is smaller than the elastic radius associated with a fully coupled explosion of the same yield and consequently, by equation (1), its low frequency coupling efficiency is lower.

The criterion for full decoupling is usually expressed in terms of a requirement that the late-time, equilibrium pressure in the cavity be less than or equal to some constant, k, times the overburden pressure. That is (Latter, et al., 1961)

$$\frac{(\gamma-1)W}{\frac{4}{3}\pi r_c^3} \leq k \rho gh \tag{2}$$

where γ is the gas constant (1.2 for air), W is the yield, r_c is the cavity radius and k is generally taken to lie in the range from 0.5 (Latter criterion) to 1.0 (Patterson criterion). Thus, the Latter criterion incorporates a safety factor of two which was designed to accommodate the large initial pressure spike which acts on the cavity wall before the cavity pressure reaches the equilibrium value given by

equation (2). We will return to consider the effects of this spike in more detail later in this report. In any case, it follows from (2) that, using this criterion, the minimum cavity radius required for full decoupling will be given by

$$r_c = \frac{2.74 \times 10^2}{(k\,\rho)^{\frac{1}{3}}} \quad \frac{W^{\frac{1}{3}}}{h^{\frac{1}{3}}} \text{ m} \qquad (3)$$

for W in kt, h in m and ρ in gm/cm^3. Thus, the cavity radius required for full decoupling is proportional to the cube-root of the yield and inversely proportional to the cube-root of the depth of burial. This is illustrated in Figure 1 which shows r_c as a function of W and h for the case k = 1, ρ = 2.0 gm/cm^3. The depth range considered extends from what is denoted "minimum containment depth" to a fixed (i.e., yield independent) upper limit of 2000 m which corresponds to a constraint (due to plastic flow) on the depth at which stable cavities can be constructed in salt. The minimum containment depth refers to the depth required for containment of a coupled explosion of yield W (i.e., approximately 122 $W^{\frac{1}{3}}$ m). Although this criterion does not apply specifically to decoupled explosions, it is probably representative of the type of conservatism an evader would have to adopt. The dashed horizontal lines on this figure denote the maximum feasible cavity radii as estimated by Evernden (1976) and Rodean (1971). Evernden's upper limit is based primarily on theoretical arguments and appears to be overly pessimistic given that the Russians have reported the existence of a free-standing, explosively-generated cavity in salt which is bigger than his upper bound (35 m vs. 30 m). Rodean's upper limit estimate, on the other hand, is empirically based and would seem to be more nearly appropriate in that it corresponds to the largest cavities which have ever been constructed by the natural gas industry using solution mining techniques in salt. However, it should be noted that these very large solution cavities are generally

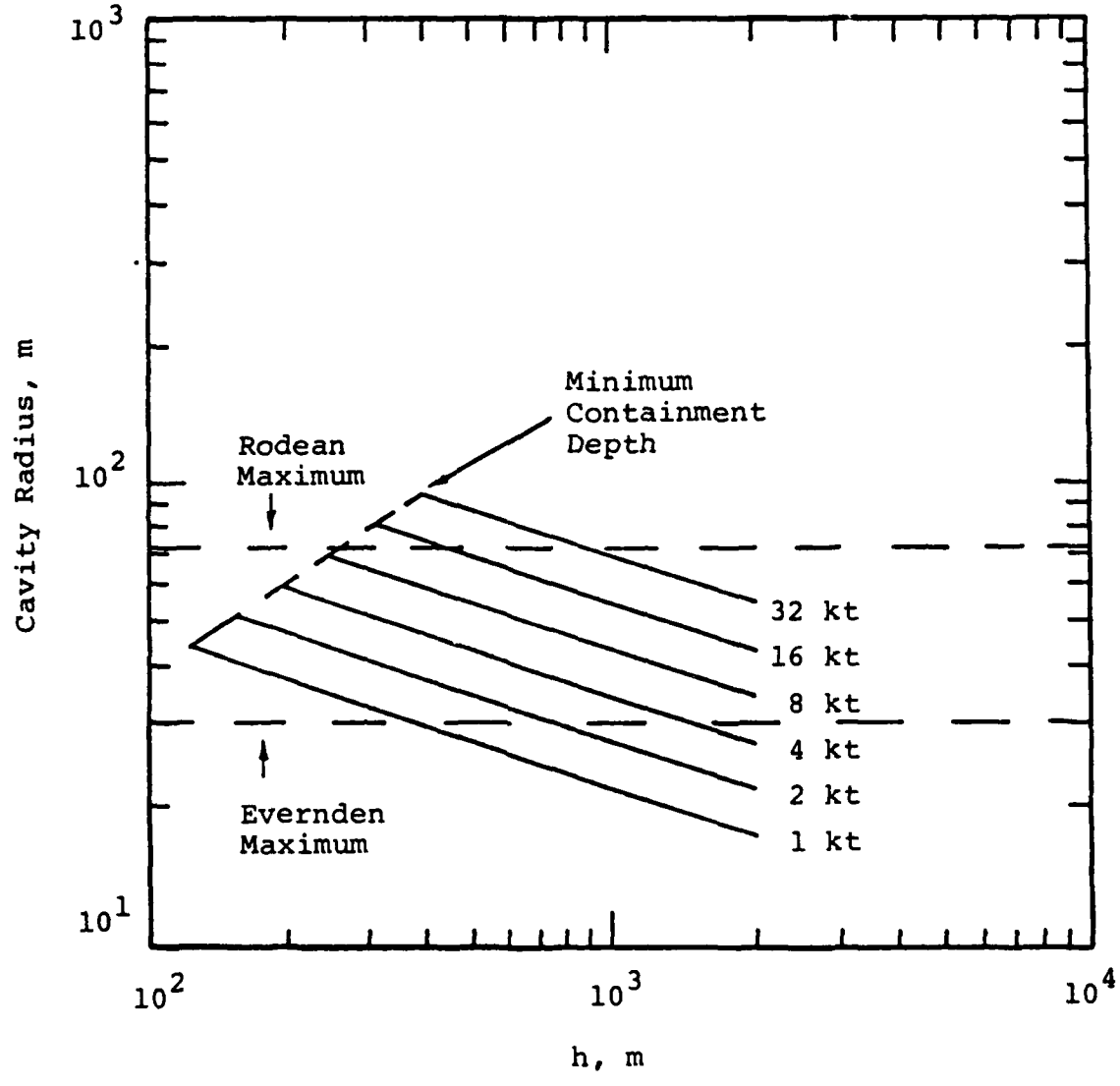

Figure 1. Cavity radii required for full decoupling as a function of source depth and yield; Patterson criteria, $\bar{\rho}$ = 2.0 gm/cm^3.

neither spherical or free-standing (i.e., they usually are filled with pressurized gas). Thus, the feasibility of constructing decoupling cavities with sizes near Rodean's upper limit has yet to be fully demonstrated. Moreover, for media other than salt, there is no evidence that free-standing cavities with radii approaching even Evernden's limit have ever been successfully constructed. Thus, there are significant practical limitations on the size of an explosion which can be fully decoupled in an underground cavity.

The simplified coupling analysis represented by equation (1) is a low frequency approximation and is not generally applicable to the high frequency seismic signals which might be detected by a regional network. The reason for this is illustrated in Figure 2 which compares estimates of the seismic source functions for coupled and fully decoupled 10 kt explosions at a depth of 828 m in salt (Murphy, 1979). It can be seen that, using these analytic approximations, both source functions are approximately flat at low frequencies and decrease as ω^{-2} above a characteristic corner frequency. Moreover, since this characteristic corner frequency is proportional to r_{el}^{-1}, it is larger for the decoupled explosion than it is for the coupled explosion. Thus, taking the ratio of these two source functions gives rise to a frequency dependent decoupling factor such as that shown in Figure 3. It can be seen that for this source approximation the decoupling factor is approximately constant up to the corner frequency of the coupled source function, above which it decreases as ω^{-2} up to the corner frequency associated with the decoupled source function. Beyond this frequency, the decoupling remains at a constant (lower) value, or at least begins to decrease less rapidly, depending on the details of the high frequency specification of the decoupled source function. This prediction that decoupling efficiency will decrease with increasing frequency constitutes one of the

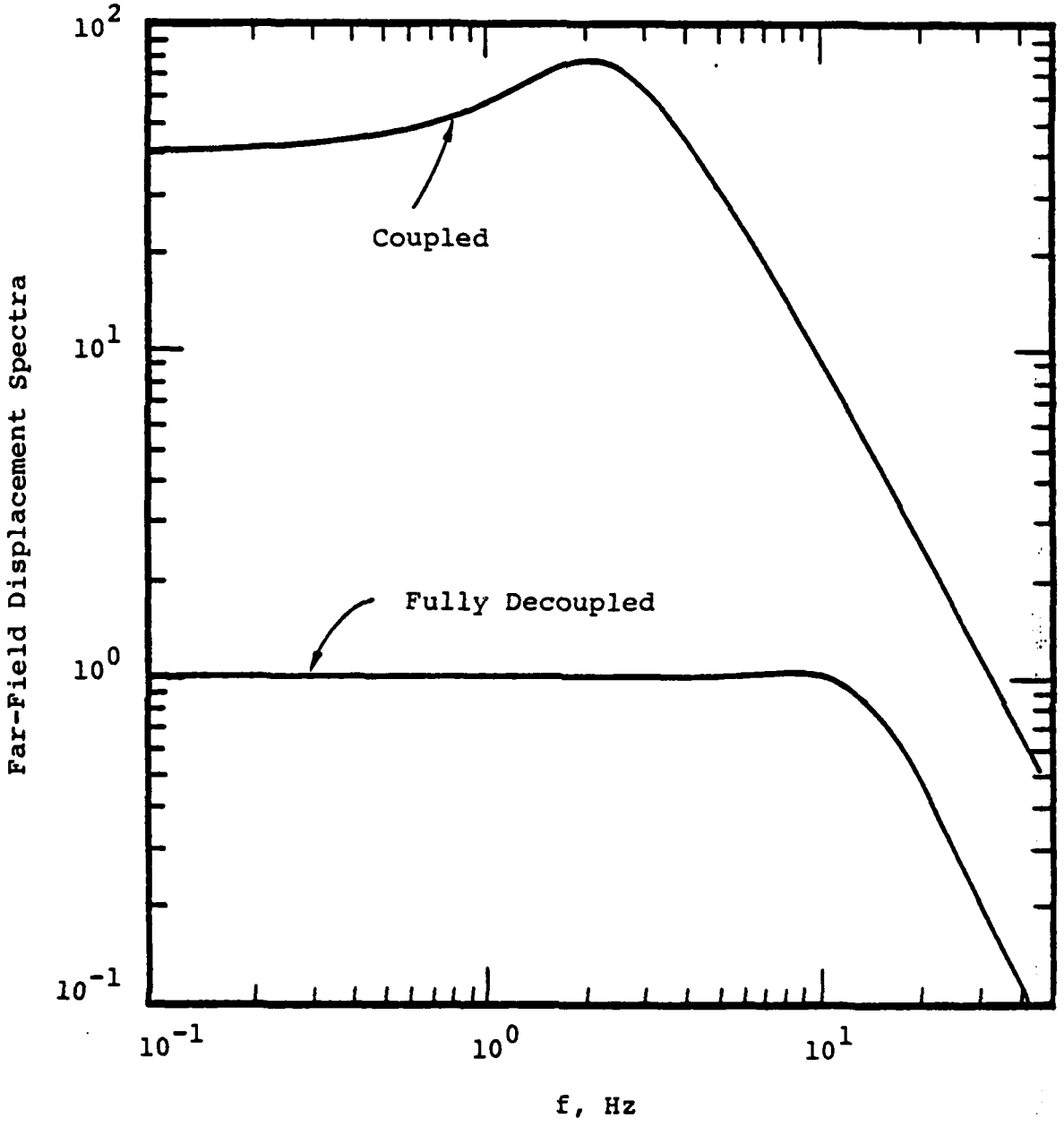

Figure 2. Comparison of theoretical coupled and fully decoupled seismic source functions, W = 10 kt, h = 828 m, SALMON salt.

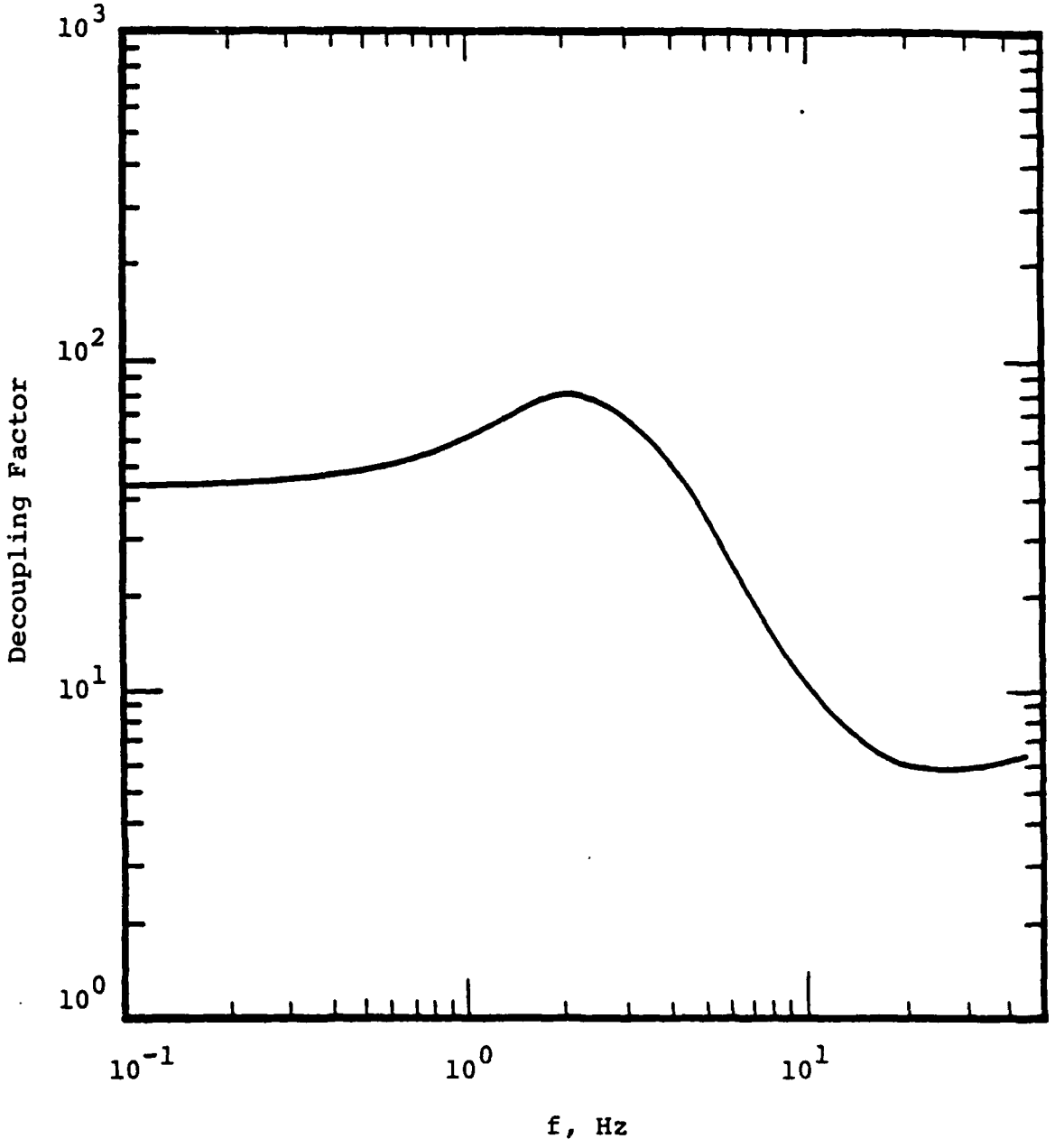

Figure 3. Predicted frequency dependent decoupling factor, W = 10 kt, h = 828 m, SALMON salt.

reasons why high frequency monitoring of such explosions appears to be attractive. On the other hand, as has been pointed out by Murphy (1979) and Evernden et al. (1986), it may be feasible for an evader to at least partially overcome this limitation and increase the decoupling efficiency at high frequencies. The reasoning that leads to this conclusion may be summarized as follows. Assume that the decoupled seismic source function can be approximated as a simple step in pressure, P H(t), acting on the wall of a cavity which is large enough to fully decouple the explosion. Then, by analogy with equation (1), it can be shown (Mueller and Murphy, 1971) that the amplitude levels of the seismic source function in the low and high frequency limits scale with the pressure level and cavity radius according to the relations

$$\lim_{\omega \to 0} |S(\omega)| \sim P\, r_c^3$$

$$\lim_{\omega \to \infty} |S(\omega)| \sim P\, r_c \qquad (4)$$

It follows that if r_c is increased by a factor k, then r_c^3 increases by a factor k^3. However, by equation (2), the equilibrium pressure in the cavity $P \sim r_c^{-3}$, so that P decreases by k^3 and the product $P\, r_c^3$ is independent of r_c. Thus, as was originally concluded by Latter et al. (1961), the low frequency decoupling effectiveness is independent of cavity radius as long as r_c is greater than the radius required for full decoupling, r_d. However, by the same line of reasoning, it can be seen from the second of equations (4) that if $r_c = k\, r_d$ $(k > 1)$, then the high frequency decoupled seismic source decreases by a factor of k^2 and, consequently, the high frequency decoupling efficiency increases by this amount. This predicted effect is illustrated in Figure 4 which shows the frequency dependent decoupling

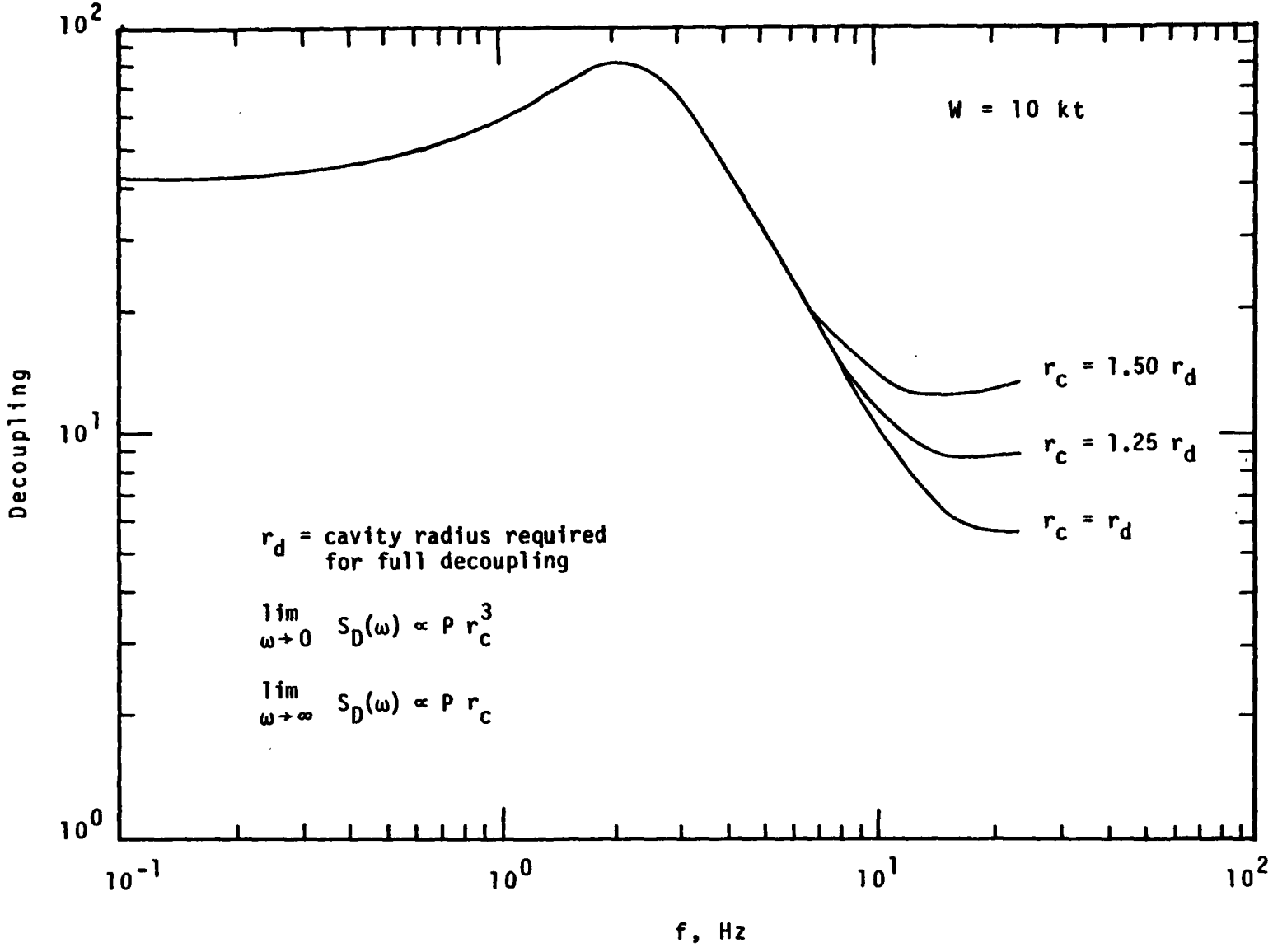

Figure 4. Predicted variation in decoupling as a function of cavity radius, W = 10 kt, h = 828 m, SALMON salt.

expected as a function of cavity radius for a 10 kt explosion in salt. Thus, the decoupling efficiency at high frequencies predicted by this simple source model can be improved somewhat at the cost of constructing a larger cavity.

In the preceding discussion we have briefly summarized the conventional wisdom concerning the seismic source characteristics of cavity decoupled explosions as represented by the analytic solution to the idealized problem of the linear, elastic response of an infinite homogeneous medium to a step in pressure in a spherical cavity. The applicability of this model at low frequencies has been verified to some extent by the limited experimental data which are available for analysis. However, it has long been recognized that this simple, low frequency approximation may not be applicable to the high frequencies of potential interest in regional seismic monitoring. For example, Figure 5 shows a comparison of the cavity pressure history computed by Patterson (1964) for a 5 kt explosion in a 51.2 m radius cavity using a nonlinear finite difference code with the simple step pressure approximation. It can be seen that the more precise finite difference solution predicts a large (nearly 1.6 kilobar) initial pressure spike on the cavity wall, followed by a rapid decay and subsequent oscillation about the steady-state value characteristic of the step function approximation. It is not clear at the present time how this complex pressure history might affect the corresponding decoupled seismic source functions, but Figure 6 shows a comparison of the seismic source functions computed from the two pressure histories of Figure 5 assuming linear, elastic response of the medium in both cases (Murphy, 1979). It can be seen that these two source estimates are roughly comparable at low frequency, but diverge significantly for frequencies above about 20 Hz. For example, the peak at about 65 Hz in Patterson's (1964) finite difference source corresponds to the inverse of the shock

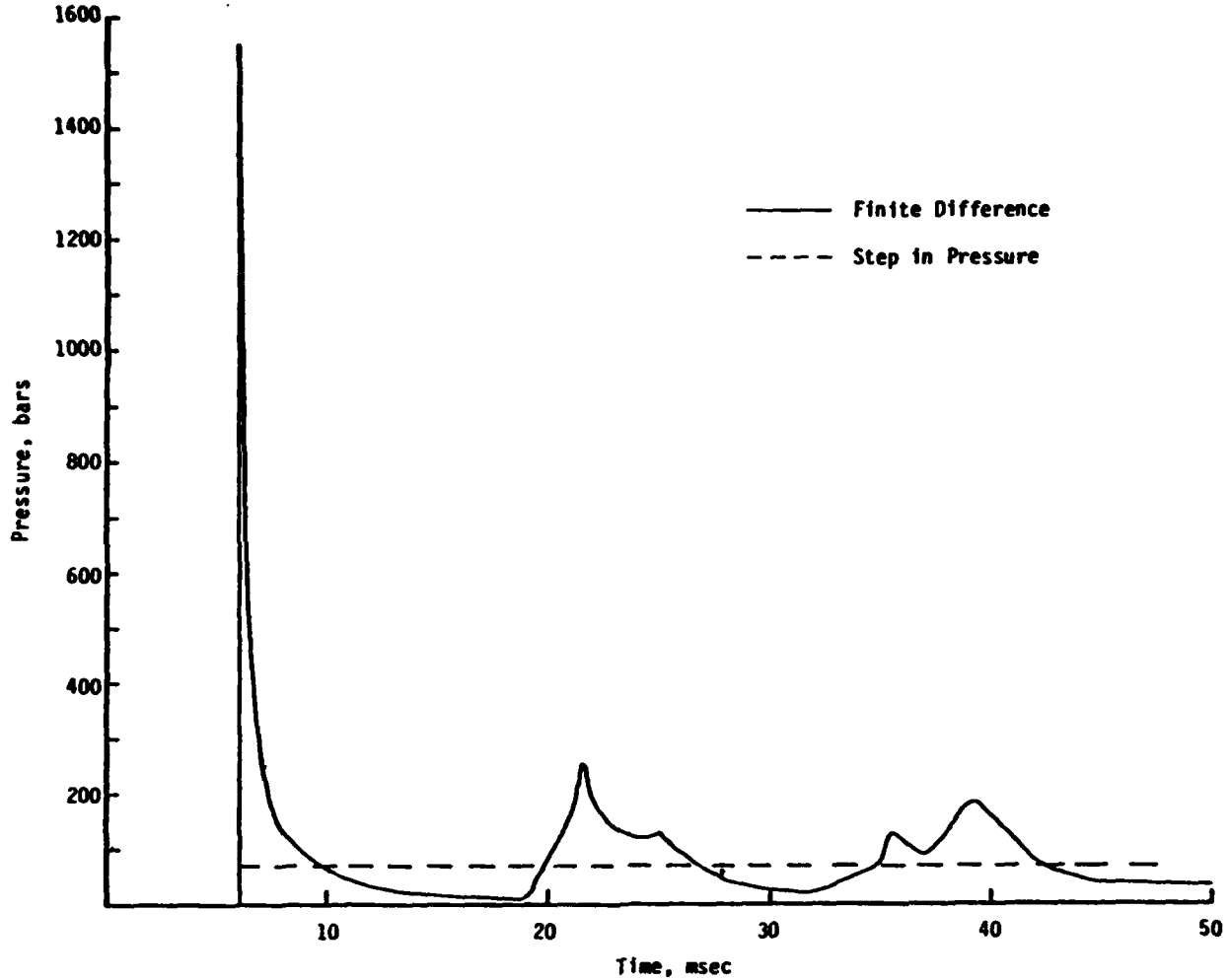

Figure 5. Pressure on cavity wall associated with a fully decoupled 5 kt explosion.

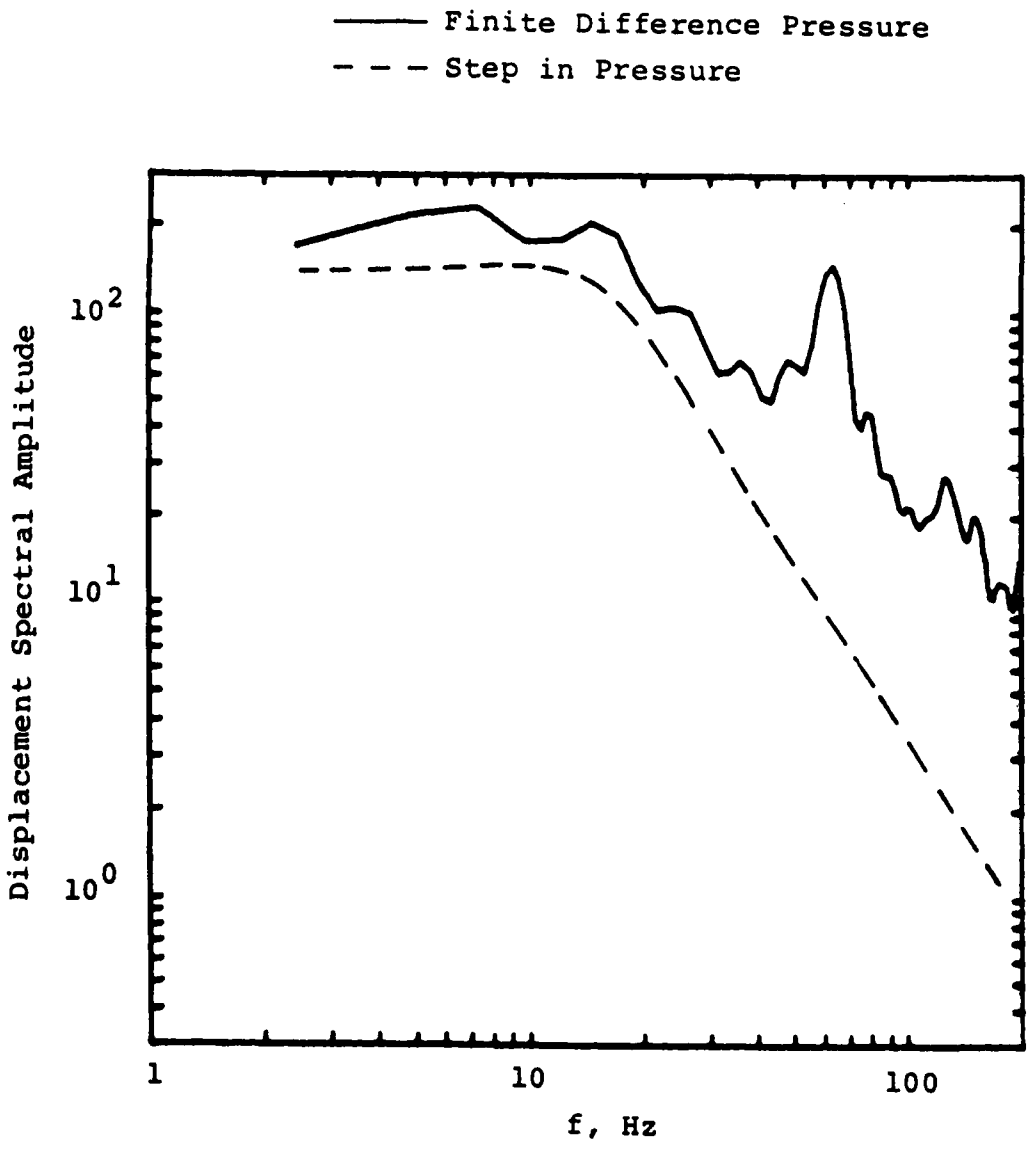

Figure 6. Comparison of decoupled seismic source approximations for a 5 kt explosion in a 51.2 m radius cavity in SALMON salt.

reverberation time in the cavity which is not accounted for in the step approximation. A more fundamental concern is that the large initial pressure spike may well induce nonlinear response in the surrounding medium which could significantly modify the solution at both high and low frequencies. This complex issue will be addressed in more detail in the following section using nonlinear finite difference simulations of a variety of decoupled seismic sources.

III. NONLINEAR FINITE DIFFERENCE SIMULATIONS OF DECOUPLED EXPLOSIONS IN SALT AND TUFF EMPLACEMENT MEDIA

It was noted in the preceding section that most previous analyses of cavity decoupling have employed the highly oversimplified step pressure approximation to describe the decoupled seismic source function. The objective of the analyses summarized in this section has been to utilize the results of detailed, nonlinear finite difference simulations of cavity decoupled explosions to better define the broadband characteristics of the seismic signals actually generated by such sources. A series of numerical simulations of decoupled explosions in unsaturated tuff and salt emplacement media have been conducted in an attempt to accomplish this objective. The experimental reference point for the tuff analysis has been the MILL YARD test conducted in a hemispherical cavity at NTS. For salt, the experimental reference point has been the STERLING test which was conducted in Mississippi in the cavity created by the SALMON explosion. In both cases, the zone size in the finite difference calculations was selected to be small enough that frequency components well above the corner frequencies of the sources were accurately represented in the solution. That is, the simulated seismic source functions are relevant to the assessment of high frequency seismic monitoring of cavity decoupled tests.

The MILL YARD experiment was conducted at NTS in an 11 m radius hemispherical cavity excavated in unsaturated tuff at a depth of 375 m. The overburden pressure at this depth is about 65 bars and, consequently, an 11 m radius spherical cavity at this depth would be expected to fully decouple an explosion in the 20 (Latter criterion) to 40 (Patterson criterion) ton yield range. Consequently, nonlinear numerical simulations of the spherical cavity problem have been conducted for both the 20 ton and 40 ton cases

using finite difference zoning fine enough to accurately represent frequency components as high as 500 Hz. The constitutive model for tuff used in these nonlinear simulations was based on the results of laboratory measurements on core samples taken from the MILL YARD test medium. Shear failure was modeled using a nonassociated flow rule with a parabolic failure surface having a stress difference at zero mean stress of 0.06 kilobars, an unconfined compressive strength of 0.10 kilobars and a maximum stress difference of 0.25 kilobars at mean stress levels above 0.30 kilobars. Based on the results of in-situ sonic logging, the P and S wave velocities were taken to be 2558 and 1372 m/sec, respectively. A detailed air equation of state was used to model the shock propagation inside of the 11 m radius cavity.

The cavity pressure as a function of time computed at a grid point near the cavity wall for the 20 ton nonlinear simulation is shown in Figure 7. It can be seen that this computed pressure profile is similar to that shown previously in Section II (cf. Figure 5) in that it is characterized by a sharp initial pressure spike associated with the reflection of the shock from the cavity wall, followed by reverberation oscillations which gradually damp out as the pressure converges to the late-time equilibrium value given by equation (2). The Fourier transform of this pressure loading is shown in Figure 8 where it is compared with that corresponding to the simple step pressure approximation. As was noted previously, the step function approximation significantly underestimates the high frequency content of the computed pressure acting on the cavity wall, particularly near the frequencies corresponding to the reverberation of the shock in the cavity.

The seismic source function computed for the 20 ton nonlinear simulation is shown in Figure 9 where it is compared with the linear elastic solution corresponding to the same cavity pressure loading. It can be seen that these two

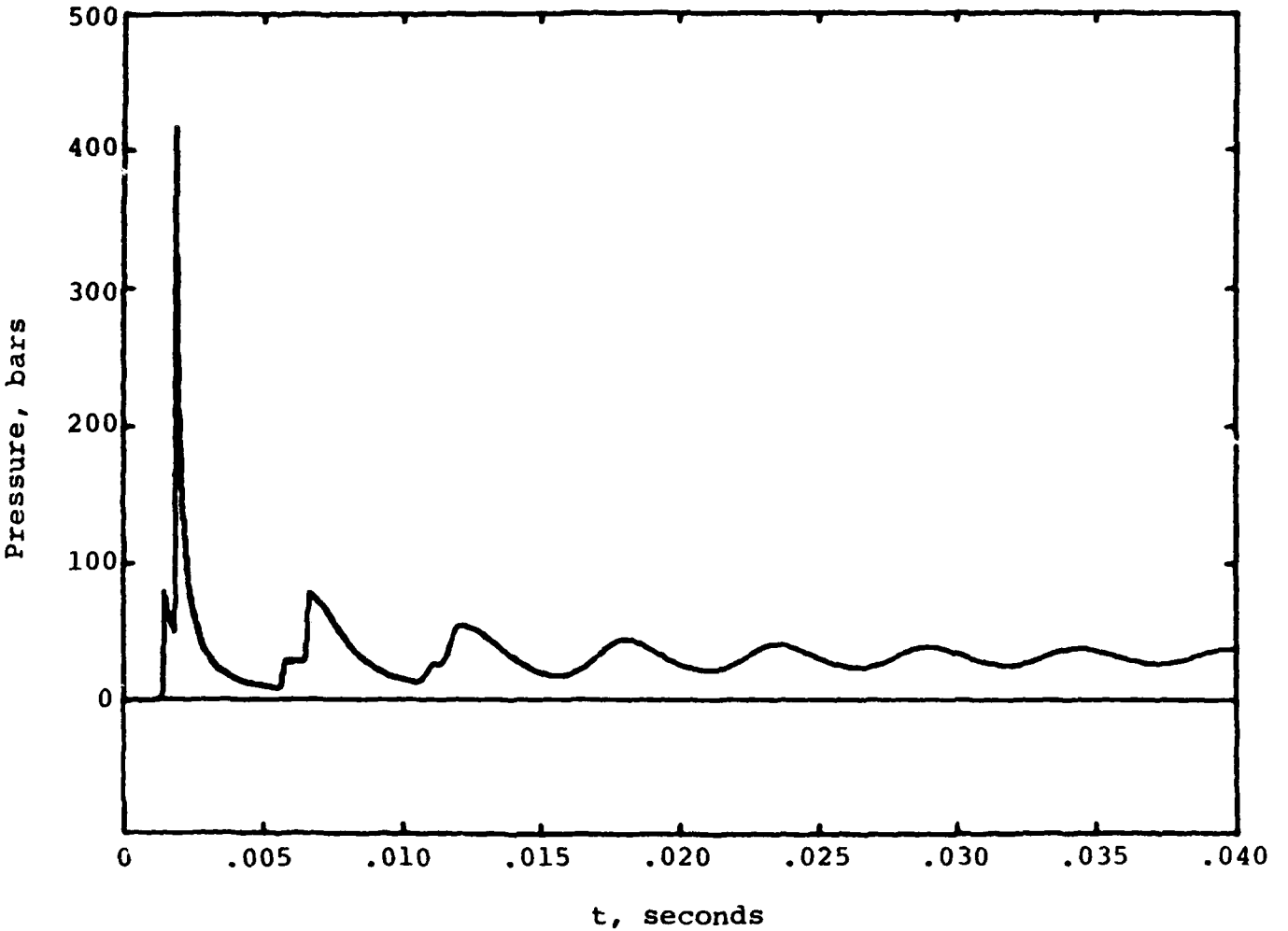

Figure 7. Computed pressure as a function of time near the cavity wall for a 20 ton nuclear explosion in an 11 m radius spherical cavity in unsaturated tuff.

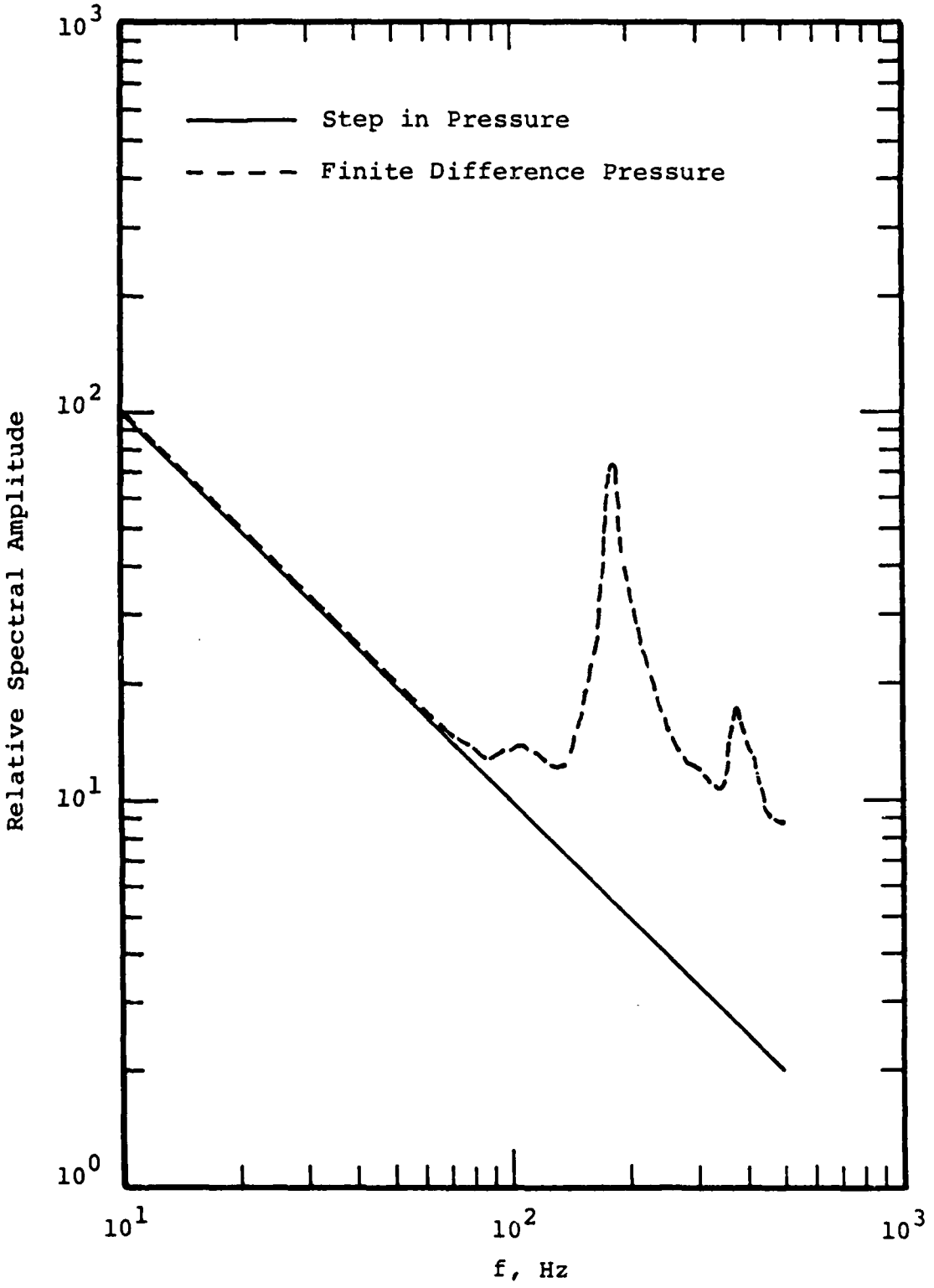

Figure 8. Comparison of the spectral composition of the complex pressure profile of Figure 7 with that associated with the simple step pressure approximation.

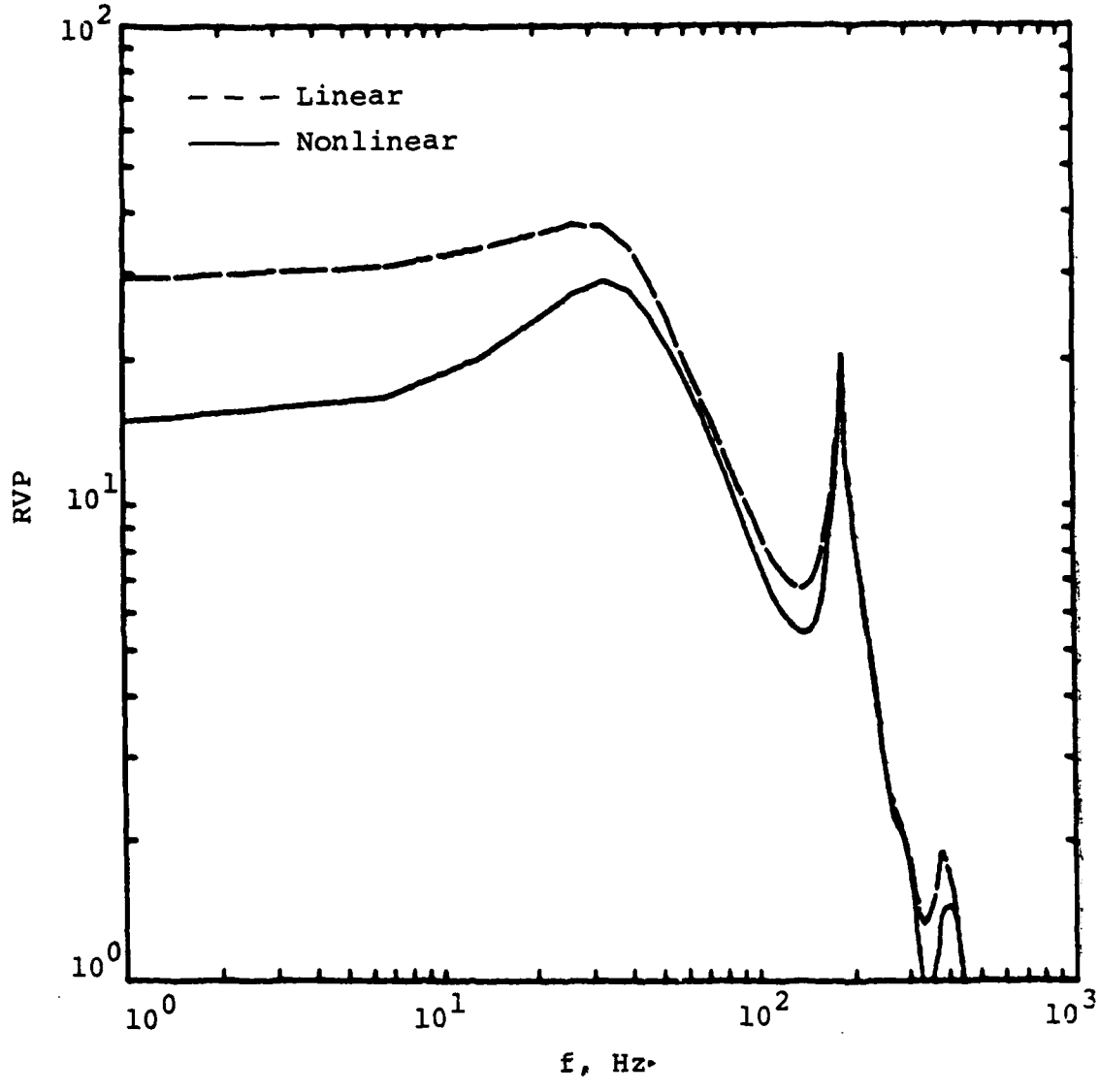

Figure 9. Comparison of linear and nonlinear seismic source functions computed for a 20 ton decoupled explosion in an 11 m radius spherical cavity in unsaturated tuff.

source functions are generally quite similar, particularly at high frequencies, with both showing corner frequencies of about 35 Hz and strong secondary reverberation peaks at around 200 Hz. Somewhat surprisingly, however, this comparison indicates increased decoupling effectiveness at low frequency in the nonlinear solution over that predicted for the linear, elastic solution, in apparent contradiction of the decoupling concept. Detailed examination of the nonlinear solution indicates that this phenomenon can be explained by the fact that in this unsaturated tuff medium, crush-up of the air filled porosity (1.8 percent) results in a decrease in the computed permanent displacement at the elastic radius and a corresponding reduction in the low frequency coupling effectiveness. In an attempt to gain more insight into the specific cause of this reduction, supplemental 20 ton simulations were performed in which the seismic source functions corresponding to the classical step pressure approximation were estimated using both the nonlinear and linear elastic models of the tuff response. In this case, the two computed source functions were found to be essentially identical and it was therefore concluded that the nonlinear reduction in low frequency seismic coupling noted in Figure 9 must be associated with the response to the initial pressure spike acting on the cavity wall. It follows that the safety factor in the Latter decoupling criterion, which was designed to accommodate this pressure spike, is not sufficient to insure linear, elastic response, at least in unsaturated, porous tuff media.

The seismic source function computed for a 40 ton explosion in the same 11 m radius spherical cavity in tuff using the nonlinear finite difference algorithm is shown in Figure 10 where it is compared with the corresponding 20 ton solution which has been multiplied by a factor of two for approximate yield normalization. This comparison indicates that the relative coupling effectiveness at 40 tons is only

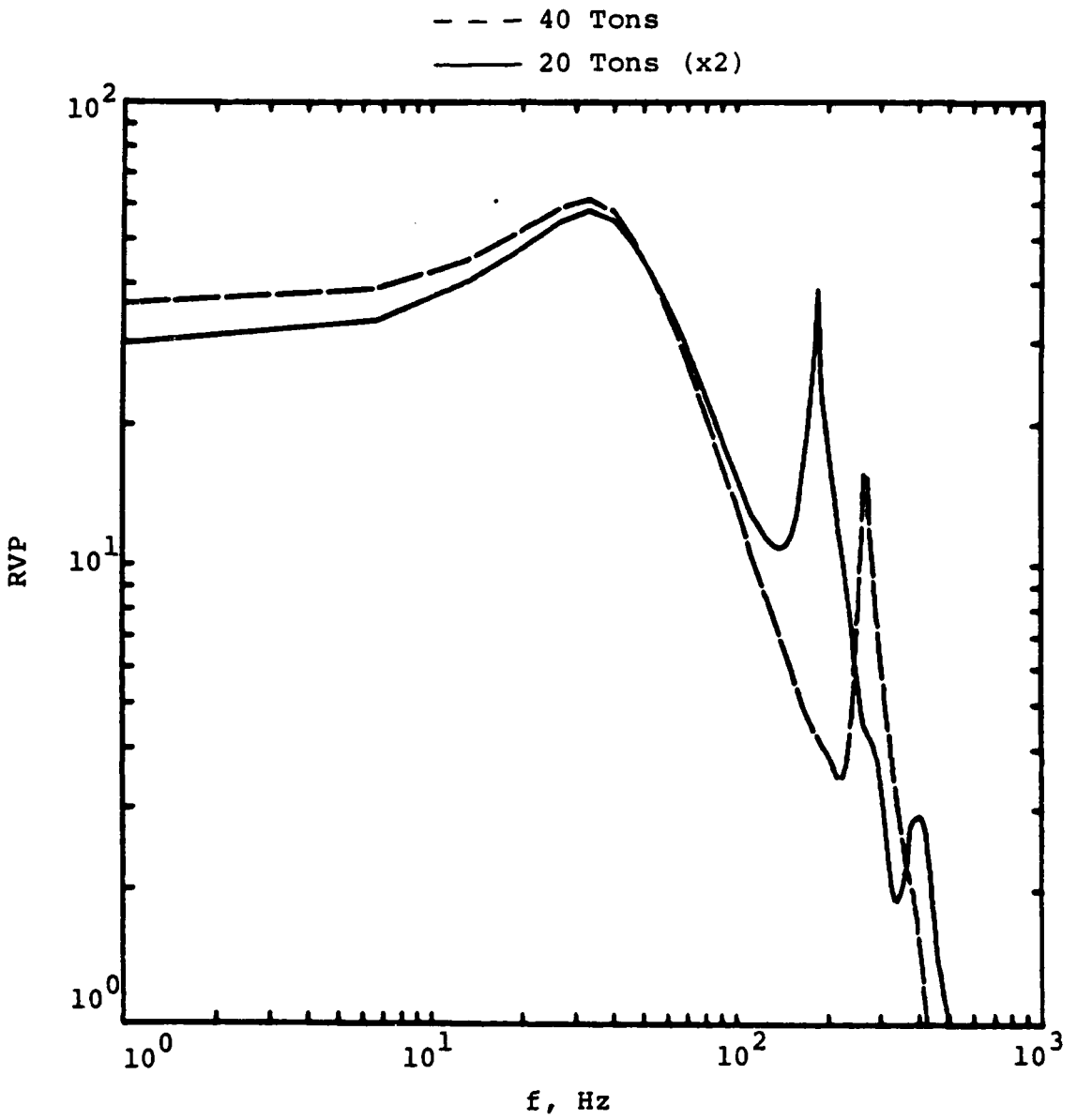

Figure 10. Comparison of 40 ton and yield-normalized 20 ton nonlinear seismic source functions computed for decoupled explosions in an 11 m radius spherical cavity in unsaturated tuff.

slightly increased at low frequency. In fact, the only significant difference between the two solutions is in the frequency of the reverberation peak which shifts to higher frequency in the 40 ton case due to the larger shock velocities. These results suggest that there is no reason to prefer the more conservative Latter decoupling criterion over that proposed by Patterson, at least for this source medium. The frequency dependent decoupling factors computed from these 20 and 40 ton simulations are shown in Figure 11 where it can be seen that, as expected, they are nearly constant at low frequency and decrease with increasing frequency above the corner frequencies associated with the corresponding coupled source functions. The principal differences with respect to the simple step function approximation are the pronounced minima in the decoupling effectiveness around 200 Hz associated with the cavity reverberation peaks. The computed decoupling levels decrease from about a factor of 40 at low frequency to values less than one above about 200 Hz. These values are low relative to those obtained from comparable simulations in salt and reflect the rapid shock attenuation which is predicted to occur in this weak tuff medium under the high pressures induced by coupled explosions. However, with respect to detectability, it is appropriate to note that the m_b values for events in dry tuff have been observed to be as much as a full order of magnitude lower than those associated with explosions of comparable yield in hardrock or saturated media. Thus, very low signal levels would be expected from small decoupled explosions in this medium.

The STERLING experiment was conducted in a salt dome in Mississippi in the cavity produced by the SALMON explosion. The cavity was approximately spherical, with a radius of about 17 m and was located at a depth of 828 m. Since the overburden pressure at this depth is about 180 bars, such a 17 m radius spherical cavity would be expected to fully decouple

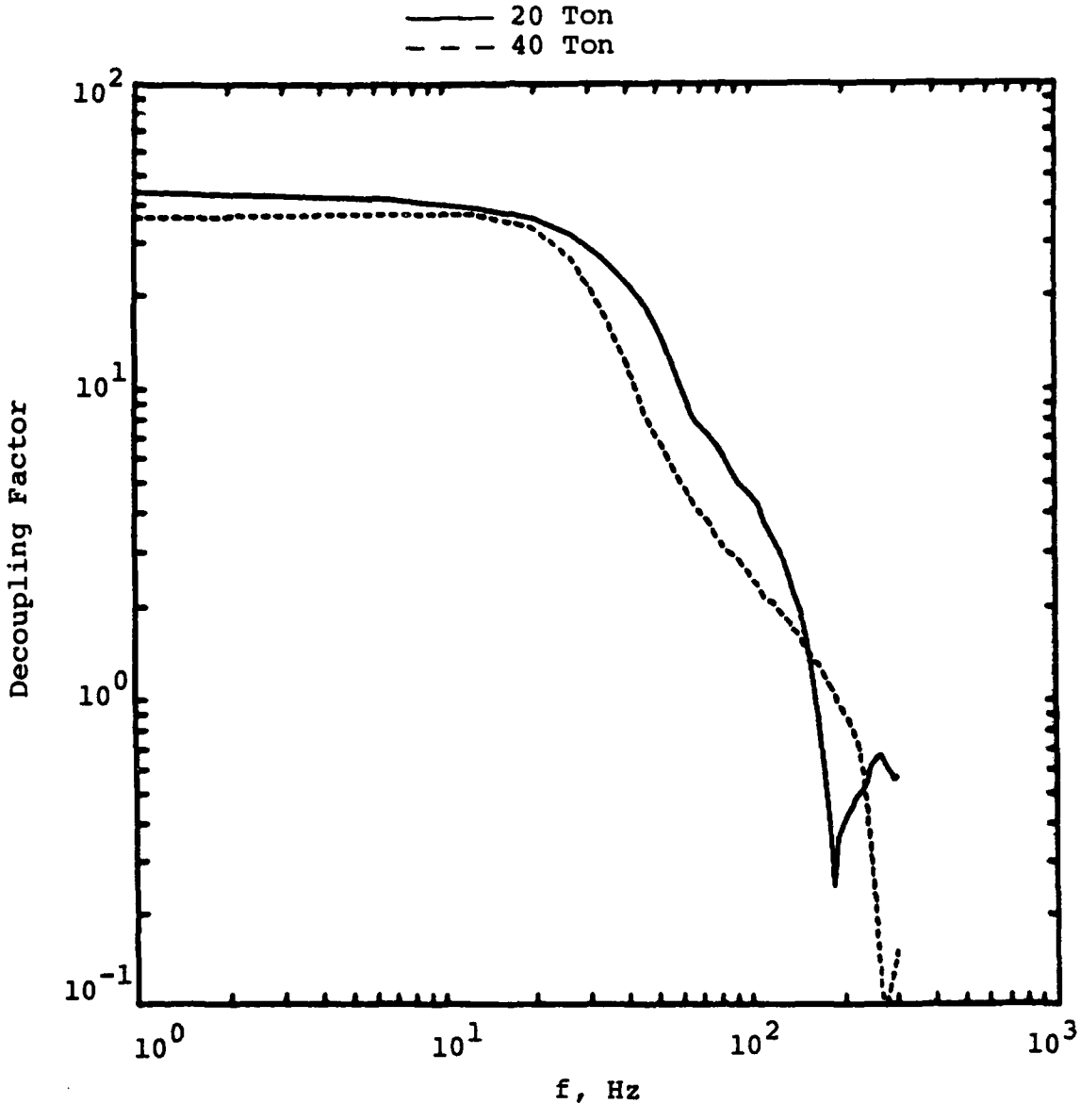

Figure 11. Comparison of frequency dependent decoupling factors computed from nonlinear simulations of 20 ton and 40 ton explosions in an 11 m radius spherical cavity in tuff.

an explosion in the 210 (Latter criterion) to 420 (Patterson criterion) ton yield range. STERLING had a yield of 380 tons, and thus was close to the Patterson limit. Consequently, a nonlinear simulation of a 380 ton nuclear explosion in a 17 m radius spherical cavity in salt was conducted in a preliminary attempt to investigate the high frequency seismic source characteristics of decoupled explosions in this medium. As in the tuff simulations, these calculations were carried out using a finite difference zoning which was fine enough to accurately represent frequency components as high as 500 Hz. The constitutive model used in these calculations was primarily based on the results of laboratory material property tests on polycrystalline salt (Heard et al., 1975). Shear failure was modeled using a nonassociated flow rule with a parabolic failure surface having a stress difference at zero mean stress of 0.14 kilobars, an unconfined strength of 0.31 kilobars and a maximum stress difference of 0.68 kilobars at mean stress levels above 0.60 kilobars. P and S wave velocities of 4551 and 2440 m/sec, respectively, were selected on the basis of analyses of SALMON free-field observations. In addition, a detailed equation of state was used to model the shock propagation inside of the 17 m radius cavity.

The cavity pressure as a function of time computed at a grid point near the cavity wall for the 380 ton explosion simulation is shown in Figure 12 where it can be seen that it is qualitatively similar to that estimated for the tuff simulation (cf. Figure 7). However, in this case the initial pressure spike has an amplitude of about 4 kilobars in contrast to the 400 bar spike amplitude of Figure 7. This reflects the fact that STERLING was conducted at much greater depth than MILL YARD and, therefore, could accommodate significantly higher pressures under the standard decoupling criteria. That is, according to these criteria, a significantly larger (i.e., 23 m radius) cavity would be required to decouple

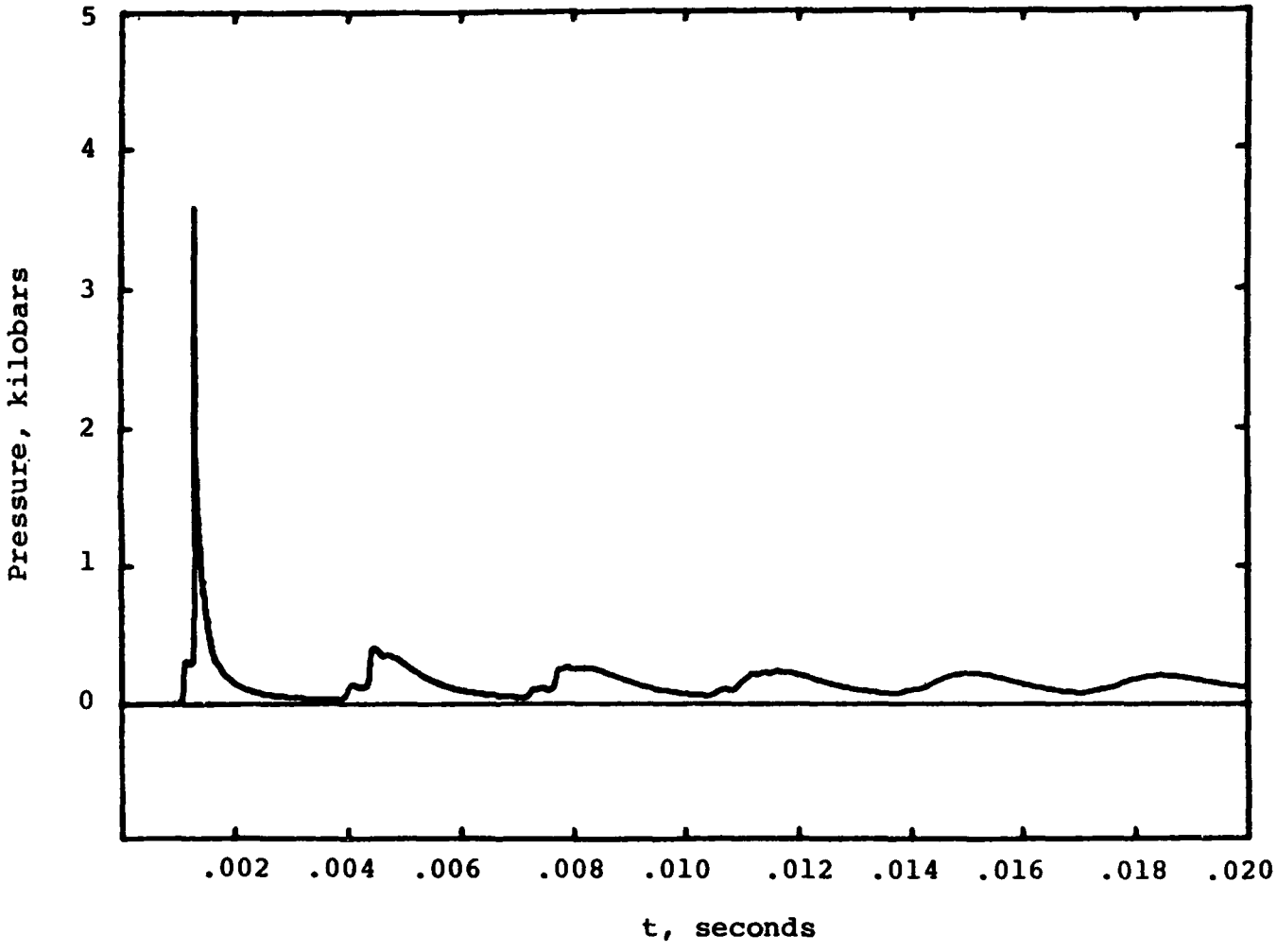

Figure 12. Computed pressure as a function of time near the cavity wall for a 380 ton nuclear explosion in a 17 m radius spherical cavity in salt.

380 tons at MILL YARD depth and, in that case, much lower peak pressures would be expected.

The seismic source function computed from the nonlinear simulation is shown in Figure 13 where it is compared with the linear elastic solution corresponding to the same cavity pressure loading. It can be seen that, as with the tuff simulations, these two source functions are quite similar at high frequencies with both showing corner frequencies of about 40 Hz and strong secondary reverberation peaks at around 300 Hz. Unlike the tuff simulations, however, the low frequency differences in this case are in accord with what would be expected from simple decoupling theory. That is, the nonlinear solution predicts slightly (~ 20 percent) greater coupling than that computed using the linear approximation. Once again, the nonlinear response is associated with the initial pressure spike on the cavity wall, as evidenced by the fact that the computed nonlinear and linear responses to the classical 160 bar step pressure loading are essentially identical. Analysis of the nonlinear simulation results indicates that the predominant nonlinear mechanism in this case was yielding of the salt out to a radius of about 19 m, as opposed to the pore crush-up mechanism which predominated in the unsaturated tuff simulations. Furthermore, comparing Figures 13 and 9 it can be seen that the effects of the nonlinearity on the seismic coupling are much less pronounced in these salt simulations and, in fact, simulations conducted with yields closer to the 210 ton limit suggested by the Latter criterion indicate little or no nonlinear response of the cavity wall. Thus, for this salt model, there is a difference between the decoupling effectiveness obtained using the Latter versus the Patterson decoupling criterion. However, the differences are confined to low frequency and do not appear to be very significant in this case.

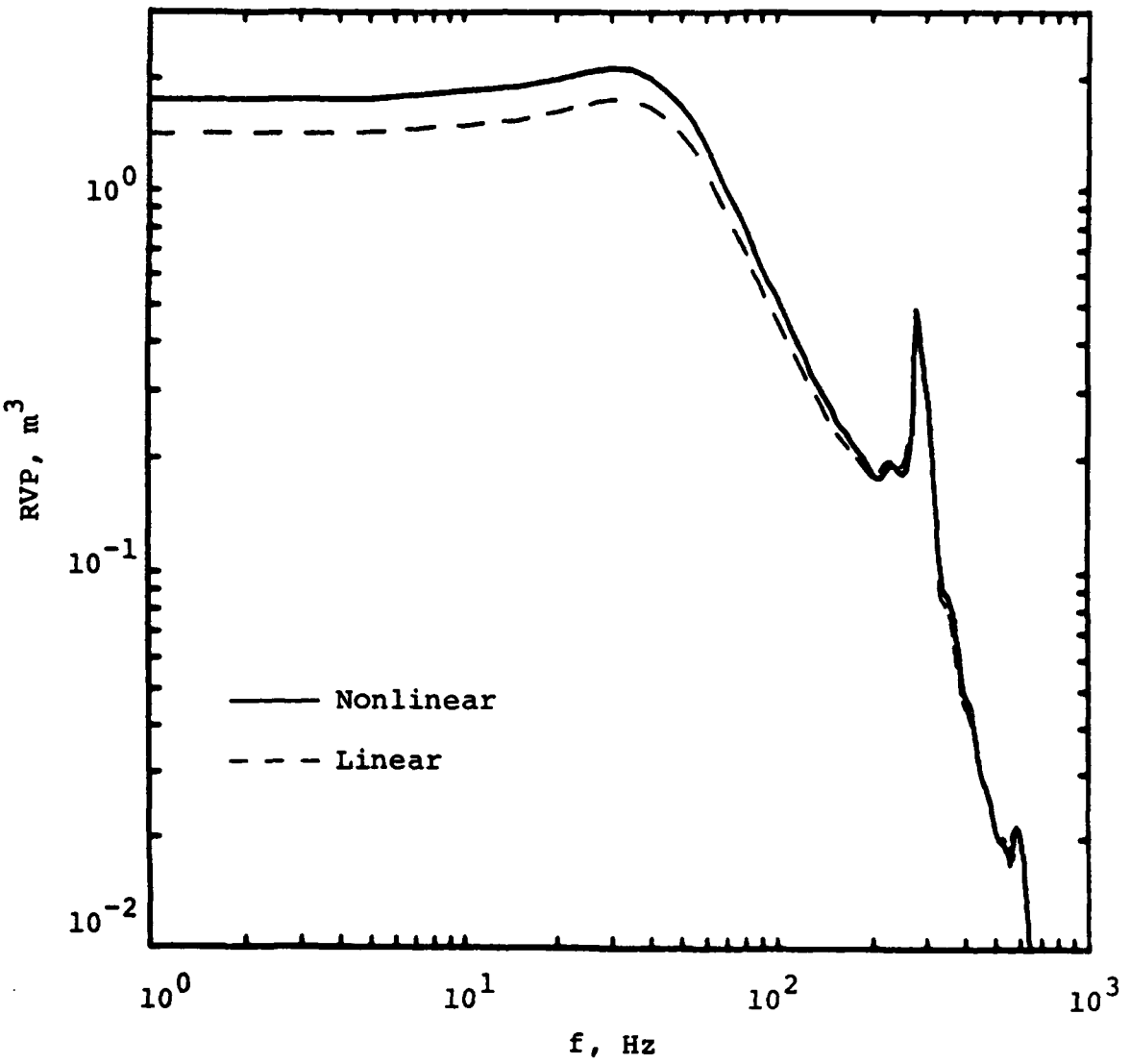

Figure 13. Comparison of linear and nonlinear seismic source functions computed for a 380 ton decoupled explosion in a 17 m radius spherical cavity in salt.

In summary, preliminary cavity decoupling simulations have been conducted for explosions in unsaturated tuff and salt emplacement media. These simulations have confirmed the fact that the simple step pressure approximation is not valid at high frequencies and that the initial pressure spike on the cavity wall can induce significant nonlinear response. However, in all the simulations conducted to date the use of the more realistic cavity pressure loading has resulted in significantly enhanced seismic coupling at high frequency over that predicted by the simple step pressure approximation. It now remains to be determined whether these predicted high frequency effects can be detected in the observed seismic data and used for identification purposes.

IV. HIGH FREQUENCY CHARACTERISTICS OF THE STERLING AND MILL YARD SEISMIC SOURCE FUNCTIONS

The results of the finite difference simulations which were described in the preceding section indicated that there may be some characteristics of the high frequency seismic source functions associated with cavity decoupled explosions which could be exploited for identification purposes. In this section, an attempt will be made to assess whether evidence of these potentially diagnostic characteristics can be identified and confidently extracted from the available experimental data. More specifically, near-field seismic data recorded from the STERLING and MILL YARD nuclear decoupling tests will be examined for evidence of these theoretically predicted high frequency source characteristics.

4.1 STERLING

STERLING was a 0.38 kt nuclear test conducted in December, 1966 in the cavity created by the SALMON explosion which had previously been detonated at a depth of 828 m in the Tatum salt dome near Hattiesburg, Mississippi. As is indicated in Figure 14, the cavity was approximately spherical with a radius of about 17 m. With reference to equation (2), 0.38 kt in a 17 m radius spherical cavity would be expected to result in a late-time equilibrium pressure level of about 160 bars, which is close to the value of the overburden pressure of 180 bars at STERLING depth. Thus, STERLING was approximately consistent with the Patterson decoupling criterion.

Most previous analyses of STERLING free-field data have focused on lower frequency recordings made at ranges of greater than 160 m. However, Sisemore et al. (1969) did report broadband results obtained from an accelerometer located near shot depth at a range of only 52 m. The radial component

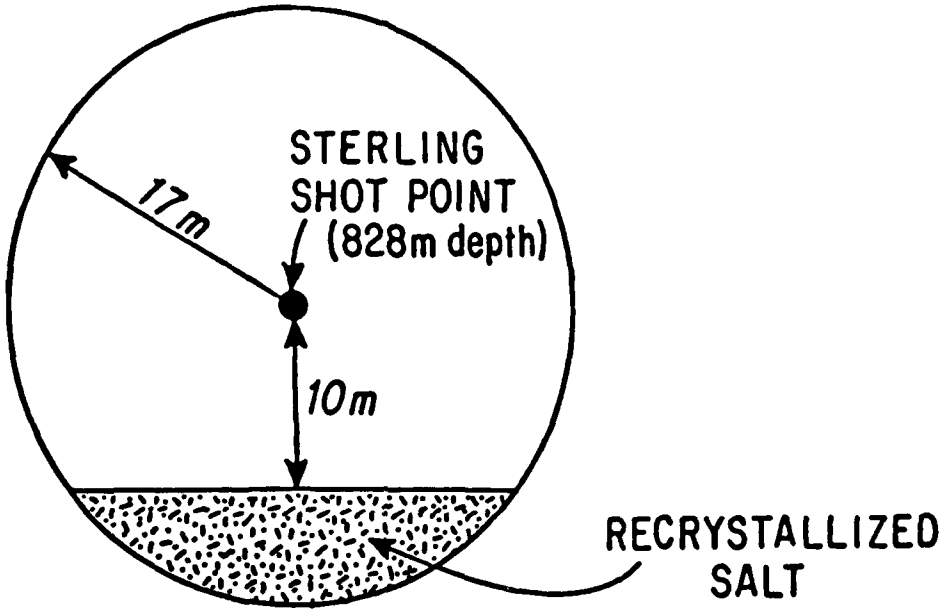

Figure 14. Cavity configuration for the STERLING decoupled explosion.

velocity time history inferred from this recording is shown in Figure 15 where it is compared with the results of two different theoretical simulations. The simulated velocity profile shown in the middle of this figure corresponds to the computed linear elastic response of the salt emplacement medium to the complex cavity pressure loading determined from a spherically symmetric finite difference calculation, while that shown at the bottom of the figure corresponds to the linear elastic response to the classical step pressure approximation. It can be seen from this comparison that even ignoring anelastic attenuation effects, the solution corresponding to the 160 bar step pressure underestimates the observed peak velocity by about a factor of three and does not match the oscillatory character of the observed velocity time history. The solution corresponding to the finite difference pressure simulation, on the other hand, provides a much better qualitative description of the observed data, although it does somewhat overpredict the peak amplitude and dominant frequency of the initial pulse. This is not surprising, since the combined effects of nonlinear and linear anelastic attenuation occurring between the cavity wall and the observation point at 52 m have been ignored in this simulation, and inclusion of any such effects would be expected to both broaden the initial pulse and reduce its amplitude. In any case, this observation provides convincing evidence that the high frequency characteristics of the actual cavity pressure loading were effectively coupled into the seismic regime in this case.

4.2 MILL YARD

The MILL YARD nuclear test was conducted at NTS on October 9, 1985 in a hemispherical cavity excavated in tuff. The cavity configuration is illustrated in Figure 16 where it can be seen that the cavity had a radius of 11 m and

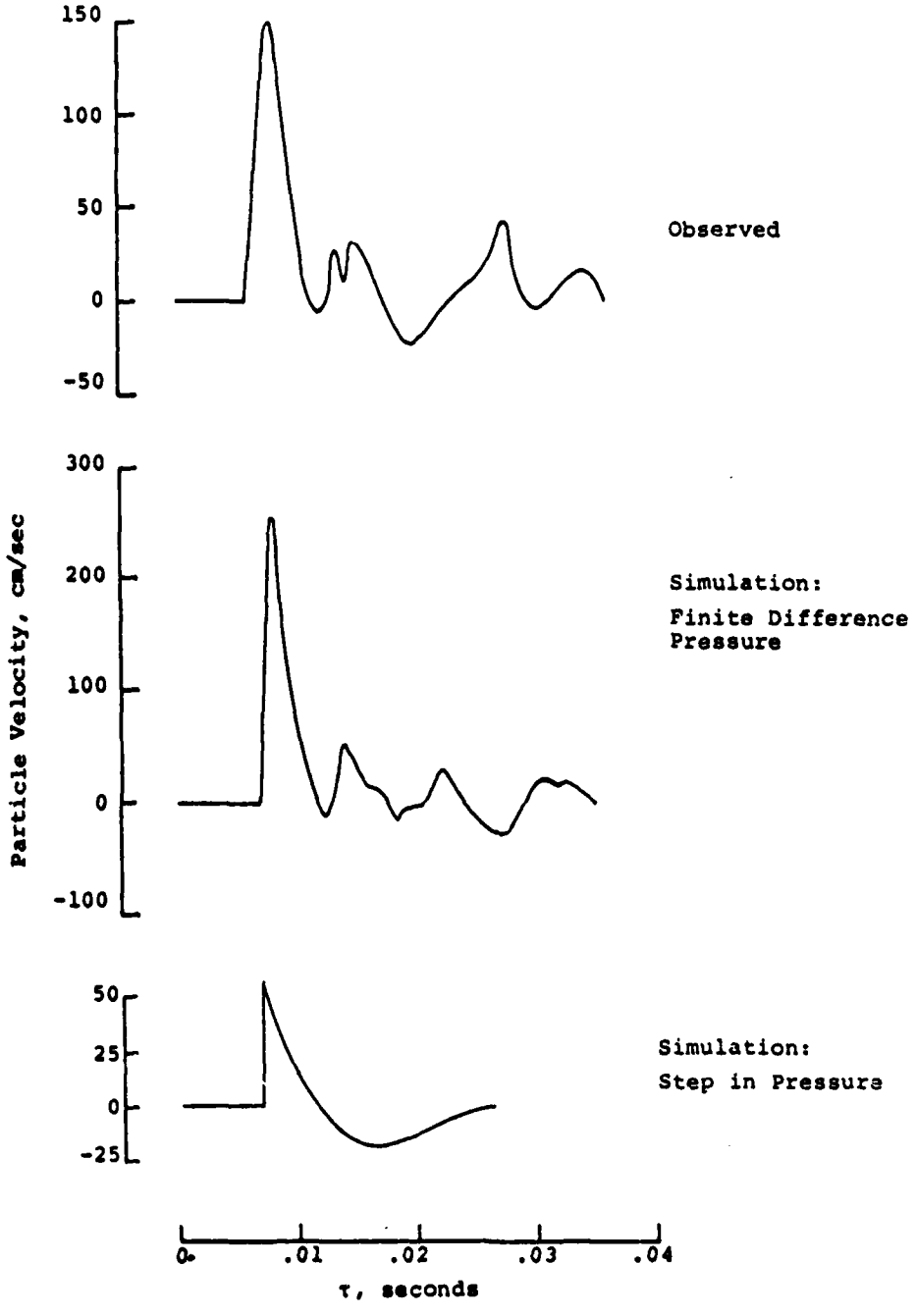

Figure 15. Comparison of the STERLING radial component velocity time history observed in the free-field at a range of 52 m with two different synthetic approximations.

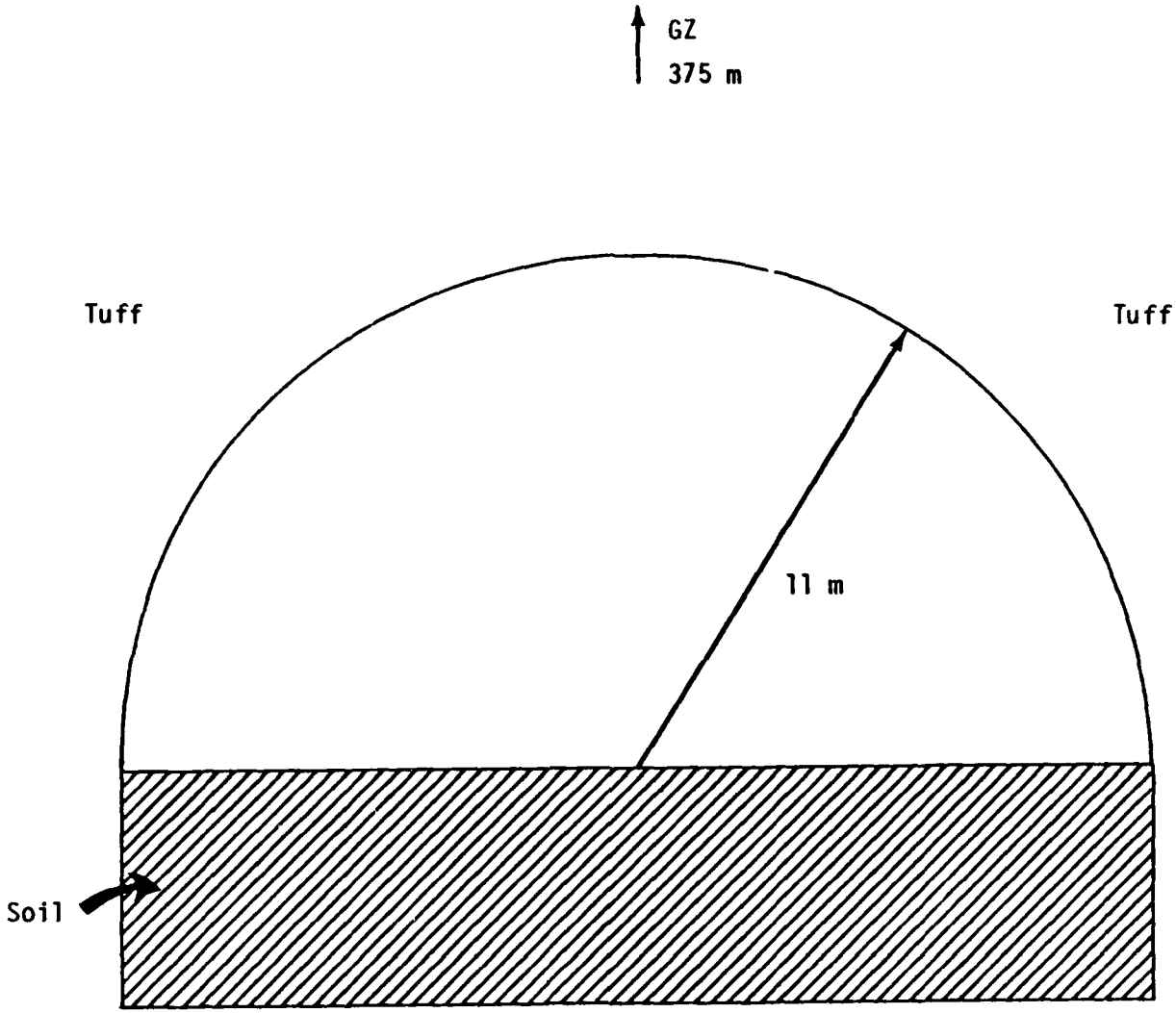

Figure 16. Cavity configuration for the MILL YARD decoupled explosion.

overlay a floor consisting of a 5 m thick layer of unconsolidated soil (Garbin, 1986). The cavity was constructed at a depth of 375 m in an unsaturated tuff medium characterized by a compressional wave velocity of about 2.5 km/sec. Figure 17 shows a vertical section through the shot point which indicates that the propagation path between the cavity and the ground surface directly above the shot (i.e., ground zero) consists of a variety of tuff layers characterized by different physical properties. Note that although there is some evidence of lateral heterogeneity, this section does not appear to be particularly complex, at least at the scale of this figure. We will return to this point later in our analysis of the characteristics of the seismic motions recorded at ground zero from MILL YARD.

Garbin (1986) analyzed both free-field and surface data recorded from this event and noted that the spectral compositions of the ground motions recorded in these two regimes are quite different. That is, the free-field data recorded at distances of about 6 and 13 m from the cavity wall are dominated by very high frequency (~ 1000 Hz) components, while those recorded at ground zero at a range of 375 m are dominated by components with frequencies of less than about 50 Hz. Garbin concluded that the MILL YARD free-field data are dominated by the motions induced by the initial pressure spike on the cavity wall. That is, as with STERLING, there is evidence that the potentially diagnostic, high frequency cavity source components do effectively couple into the seismic regime. However, the lower frequency content of the surface recordings indicates that frequency dependent attenuation can mask these source characteristics, even over relatively short propagation paths. This observation motivated a more detailed analysis of the spectral composition of the MILL YARD surface recordings.

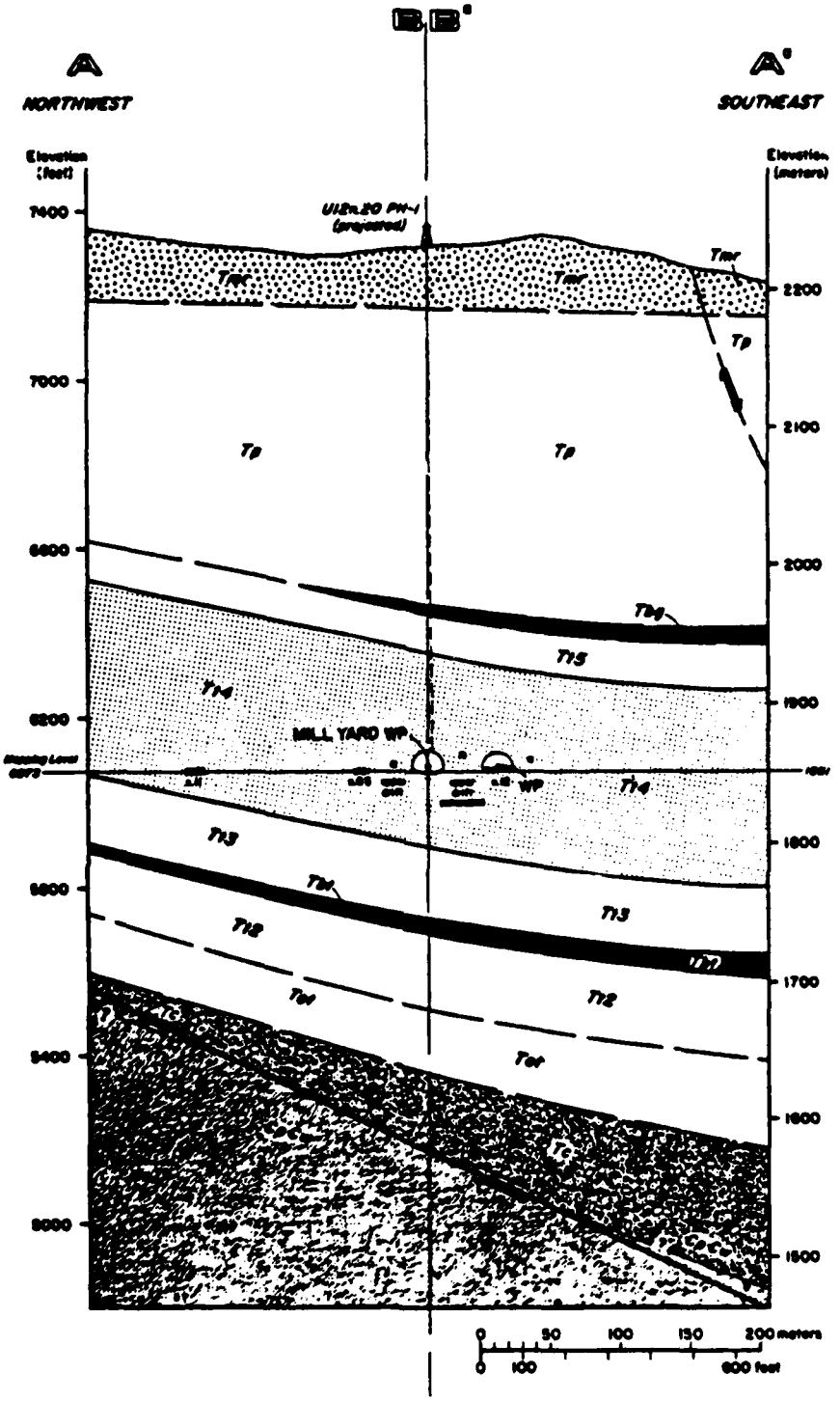

Figure 17. Representative vertical cross-section through the MILL YARD cavity.

The initial P wave displacement spectrum derived from the vertical component ground motion recorded at ground zero is shown in Figure 18 where it is compared with the spectrum predicted theoretically for a step in pressure in an 11 m radius spherical cavity in a medium characterized by a compressional wave velocity of 2.5 km/sec. It can be seen that while there is evidence of some potentially interesting high frequency complexity in this observed spectrum, the most notable features of this comparison are the facts that the observed corner frequency is lower than expected and the spectral decay above the corner frequency is much more rapid than that predicted by the simple elastic solution. It was originally thought that these discrepancies might be related to the hemispherical geometry of the MILL YARD cavity. However, subsequent investigation has provided strong evidence that these two spectra can, in fact, be reconciled within the context of a fairly simple propagation path model.

The first step in the analysis was to estimate and correct for the effects of anelastic attenuation. This was accomplished using a model in which it was assumed that the P wave displacement source function should decrease approximately as ω^{-2} above the source corner frequency and that the frequency dependent attenuation effects of propagation could be accounted for by a conventional, constant Q operator. Application of this model to the observed P wave spectrum of Figure 18 leads to an estimated average Q value of about 10 for the path between the cavity surface and ground zero. Figure 19 shows the comparison with results from applying this attenuation correction to the observed spectrum of Figure 18. It can be seen that the Q-normalized observed spectrum is fairly consistent with the simple theoretical prediction, although there remain some significant spectral modulation effects which are not accounted for by the model. Analysis of the corresponding time domain signals provides insight

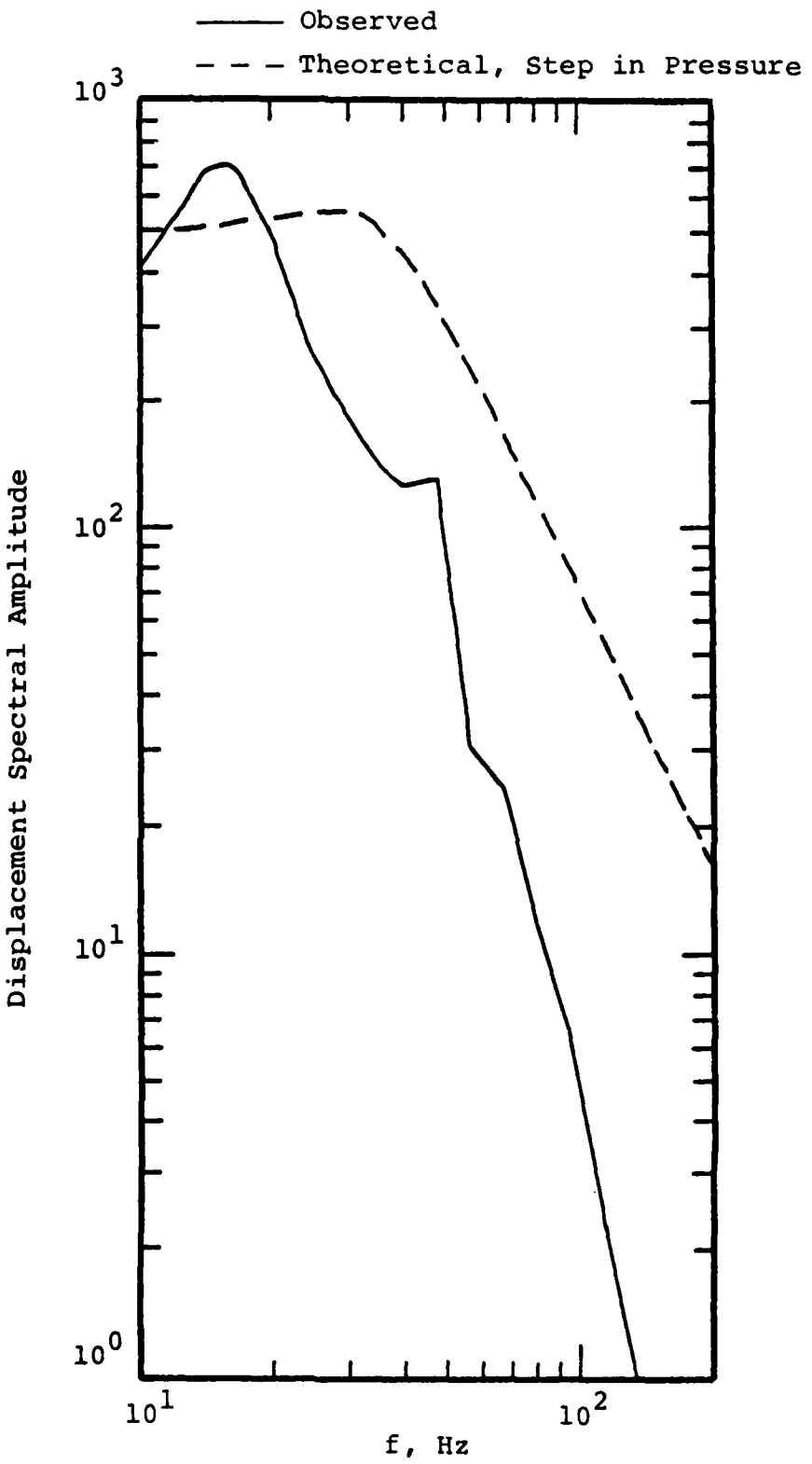

Figure 18. Comparison of the observed MILL YARD ground zero P wave displacement spectrum with the spectrum predicted theoretically for a step in pressure in an 11 m radius spherical cavity.

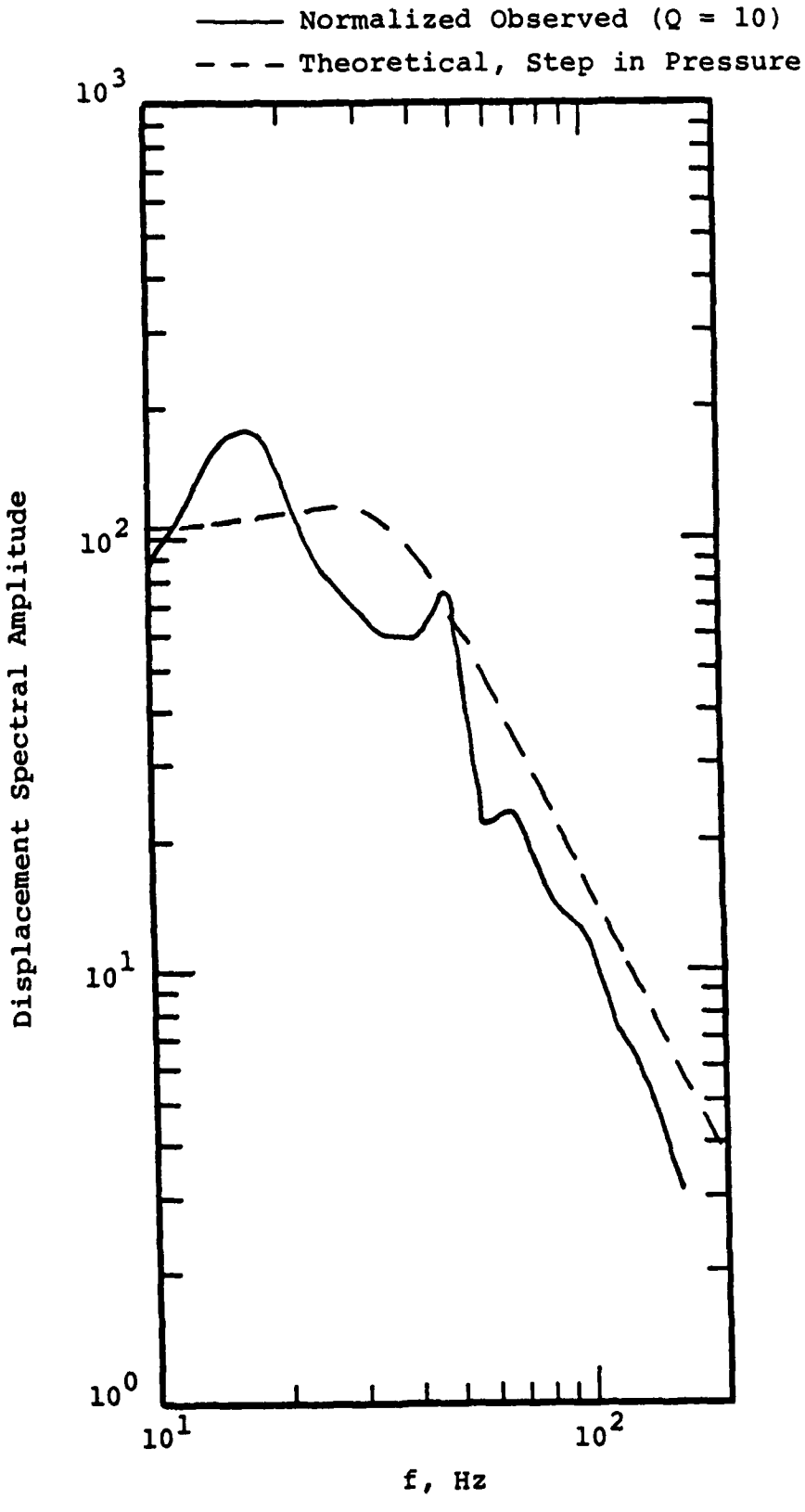

Figure 19. Comparison of the attenuation normalized, MILL YARD ground zero P wave displacement spectrum with the spectrum predicted theoretically for a step in pressure in an 11 m radius spherical cavity.

into the cause of this spectral complexity. For example, Figure 20 shows comparisons between the observed ground zero acceleration, velocity and displacement waveforms with the vertical component synthetics predicted using the simple spherical cavity source model and an anelastic propagation model characterized by a Q value of 10. It can be seen from this figure that the dominant periods of the first half cycles of the observed acceleration and velocity waveforms are matched quite well by these synthetics, indicating that the inferred combination of source and Q models is approximately correct. However, the displacement comparison is less satisfactory and examination of the acceleration and velocity comparisons suggests that this may be due to interference with a secondary phase of opposite polarity arriving about 0.03 seconds after the first motion. The onset of this arrival is indicated by the vertical arrows above these traces and its phase relationship to the first arrival is most clearly indicated in the comparison of the observed and synthetic velocity waveforms. These observations suggest that the modulation evident in the observed displacement spectrum of Figure 19 may be due to interference between arrivals. In fact, the observed short time delay and phase relationship between the arrivals is suggestive of a near-surface reverberation effect. The plausibility of this interpretation is demonstrated more clearly in Figure 21 where the result of dividing the attenuation corrected spectrum of Figure 19 by the source spectrum corresponding to the step in pressure in the 11 m radius spherical cavity is displayed and compared with theoretical layer response functions computed assuming a two-way travel time in the layer consistent with the observed interference pattern and layer Q values of ∞ and 10 respectively. Thus, for example, if the near-surface compressional wave velocity is 1000 m/sec, then the observed delay time of 0.03 seconds would imply a layer thickness of about 15 m, which is not an

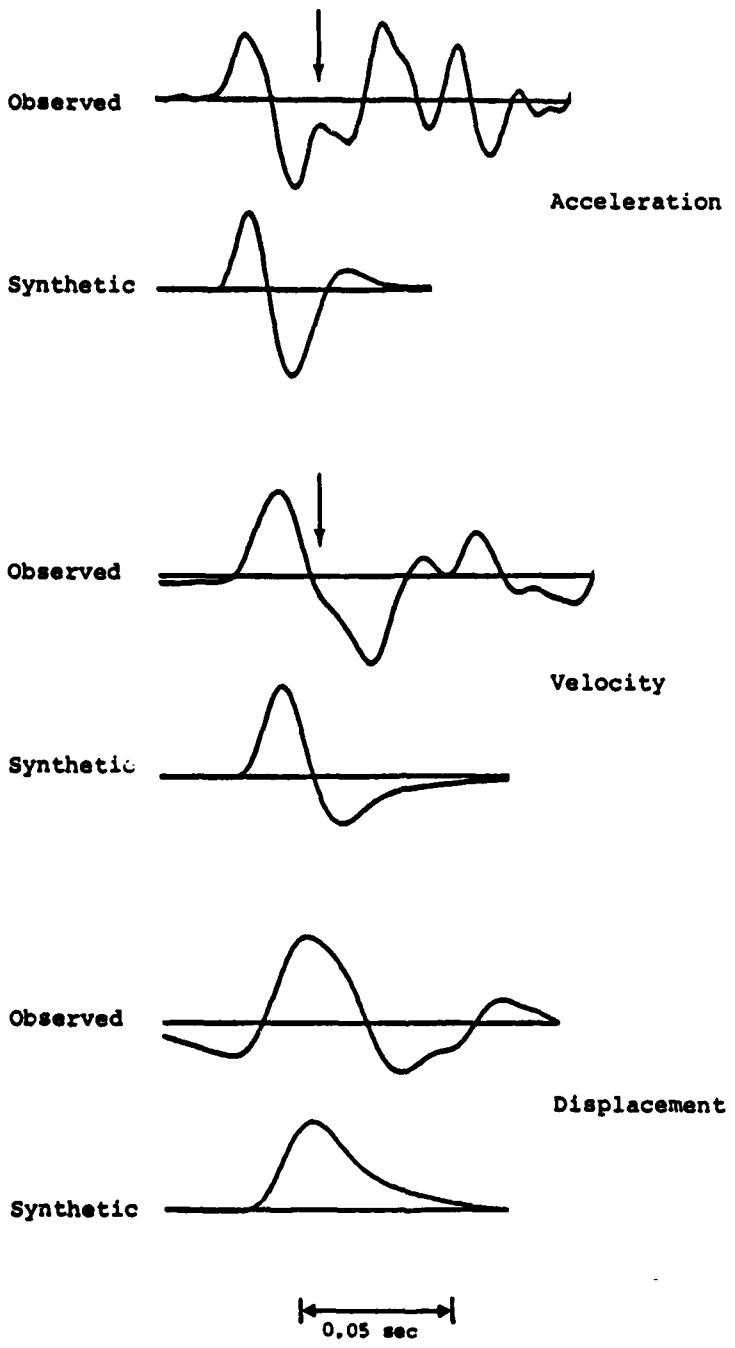

Figure 20. Comparison of observed MILL YARD ground zero acceleration, velocity and displacement waveforms with the vertical component synthetics predicted using the simple spherical cavity source model and an anelastic propagation model with Q = 10.

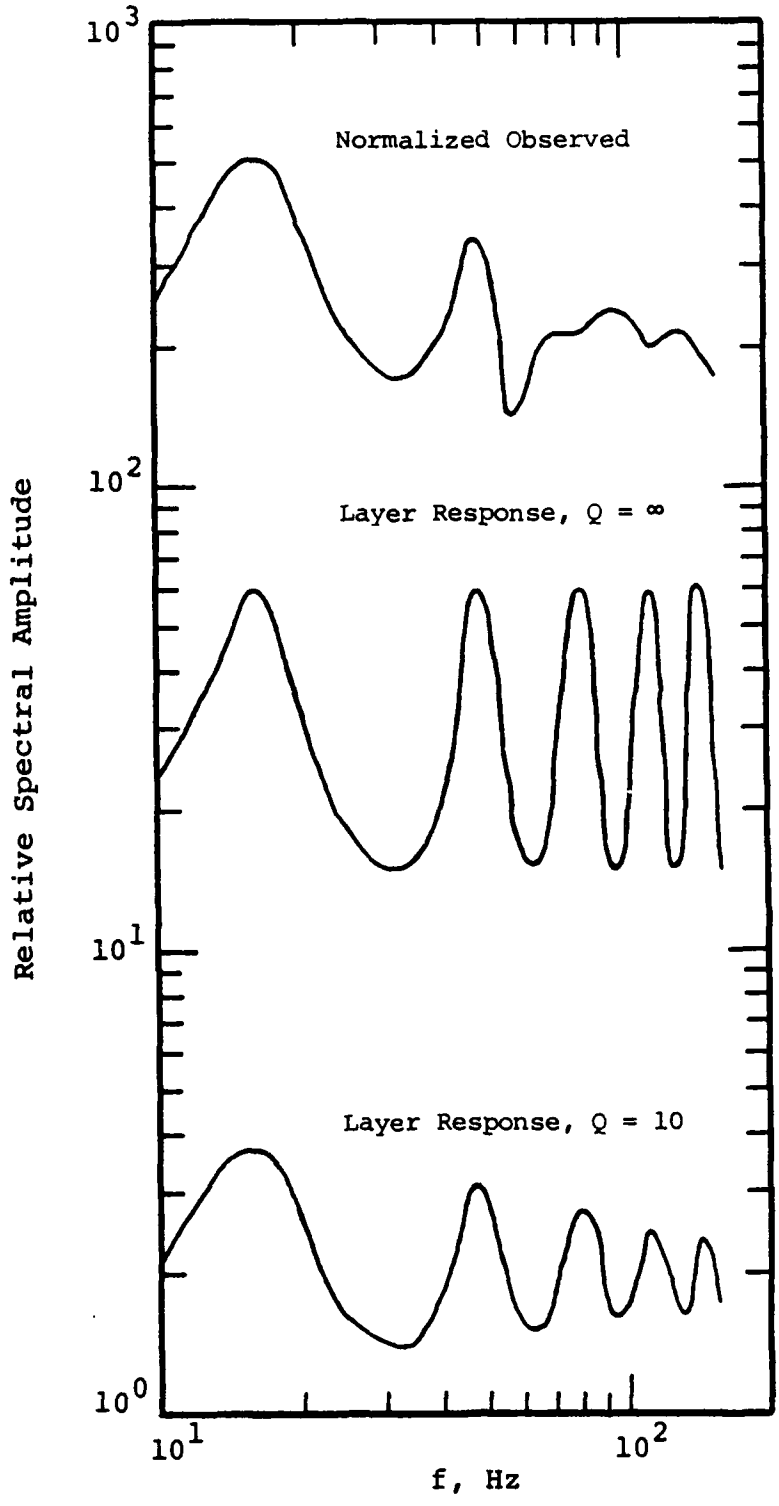

Figure 21. Comparison of source and attenuation corrected MILL YARD ground zero displacement spectrum (top) with theoretical layer response functions computed assuming Q values of ∞ (center) and 10 (bottom).

unreasonable value. It can be seen from this figure that the Q = 10 theoretical layer response agrees quite well with the normalized observed spectrum below about 80 Hz. The extent to which this model fits the time domain data is illustrated in Figure 22 where the comparison shown previously in Figure 20 has been modified to incorporate the effect of this Q = 10 layer response into the synthetics. It can be seen that these initial portions of the acceleration, velocity and displacement synthetic waveforms are now in excellent agreement with the observations, confirming the applicability of the inferred site response model. Finally, Figure 23 shows the comparison between the attenuation-normalized observed spectrum and the theoretical spectrum obtained by multiplying the step function solution times the layer response function. This comparison seems to confirm the fact that the MILL YARD P wave source function can be adequately approximated by a simple step in pressure in an 11 m radius spherical cavity, at least over this limited frequency range. That is, as was suggested by the finite difference simulations described in the previous section (cf. Figure 10), higher frequency data will be required to confidently identify the effects of the pressure spike and reverberations in the MILL YARD cavity. Unfortunately, the high degree of anelastic attenuation occurring along the propagation path to ground zero does not allow us to recover this high frequency information in this case.

It follows from the above discussion that very detailed path corrections will be required if high frequency seismic data are to be used to identify small decoupled explosions. Another example of the complexity of such propagation effects is provided by Figure 24 which shows the vertical and two horizontal components of displacements, velocity and acceleration recorded at ground zero from MILL YARD. In each case, the three orthogonal components of motion are plotted at the same absolute amplitude scale so that the

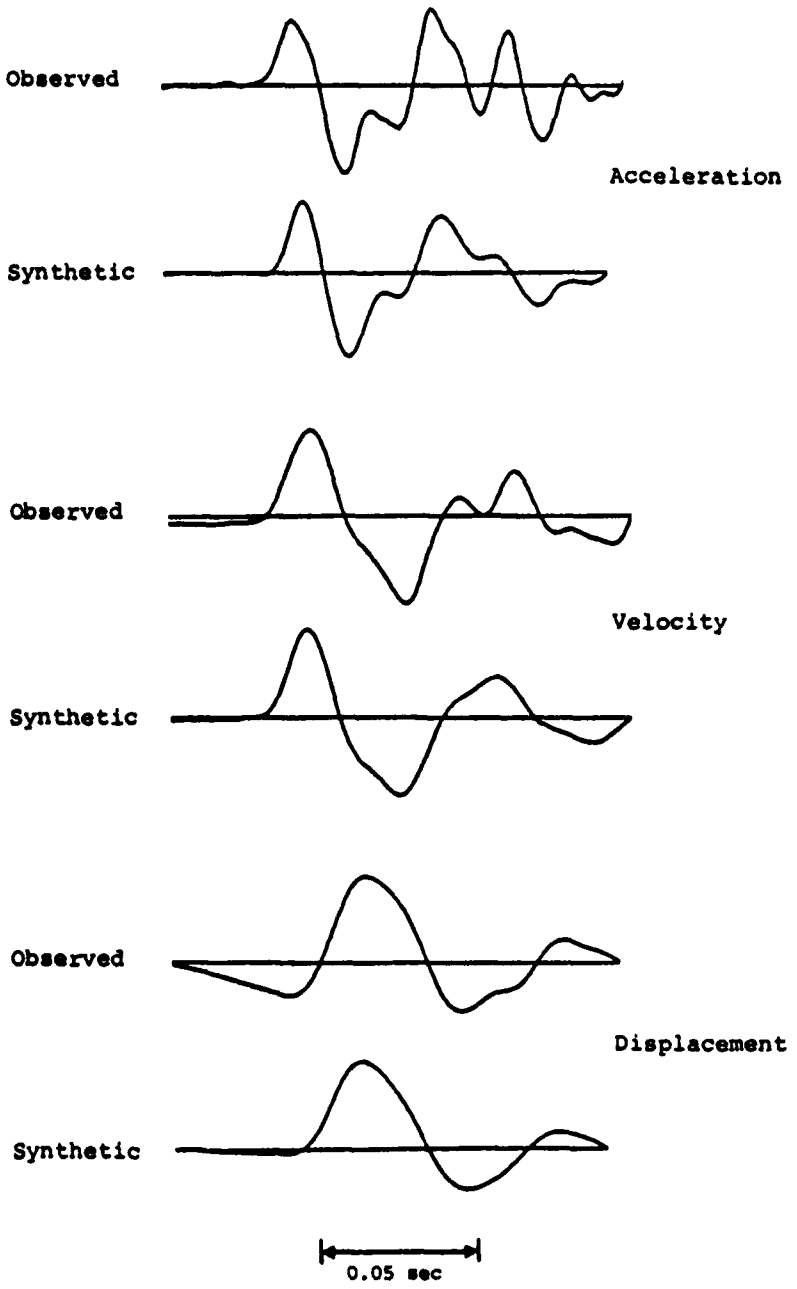

Figure 22. Comparison of observed MILL YARD ground zero acceleration, velocity and displacement waveforms with the vertical component synthetics computed by convolving the synthetics of Figure 20 with the Q = 10 layer response function from Figure 21.

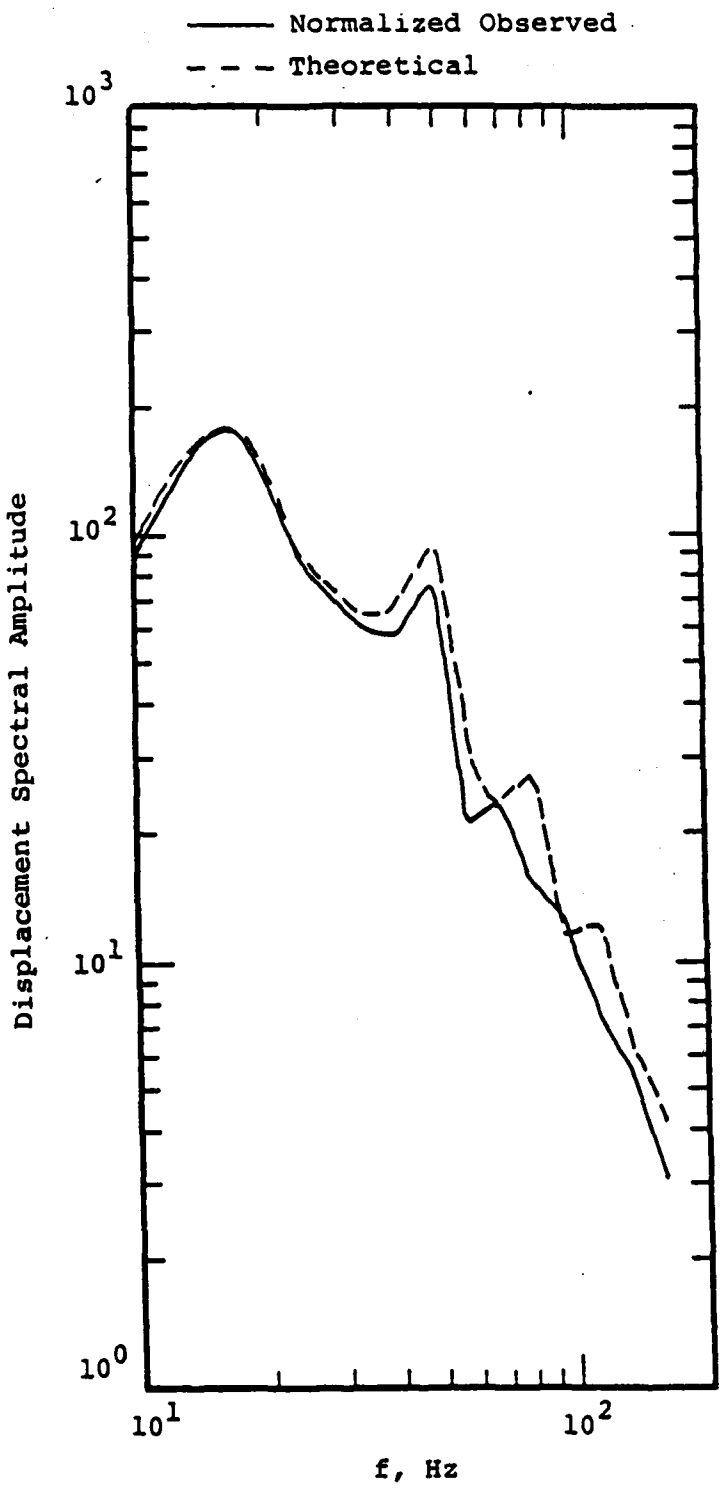

Figure 23. Comparison of the attenuation-normalized, MILL YARD ground zero P wave displacement spectrum with the theoretical spectrum obtained by multiplying the step function solution of Figure 18 times the Q = 10 layer response function from Figure 21.

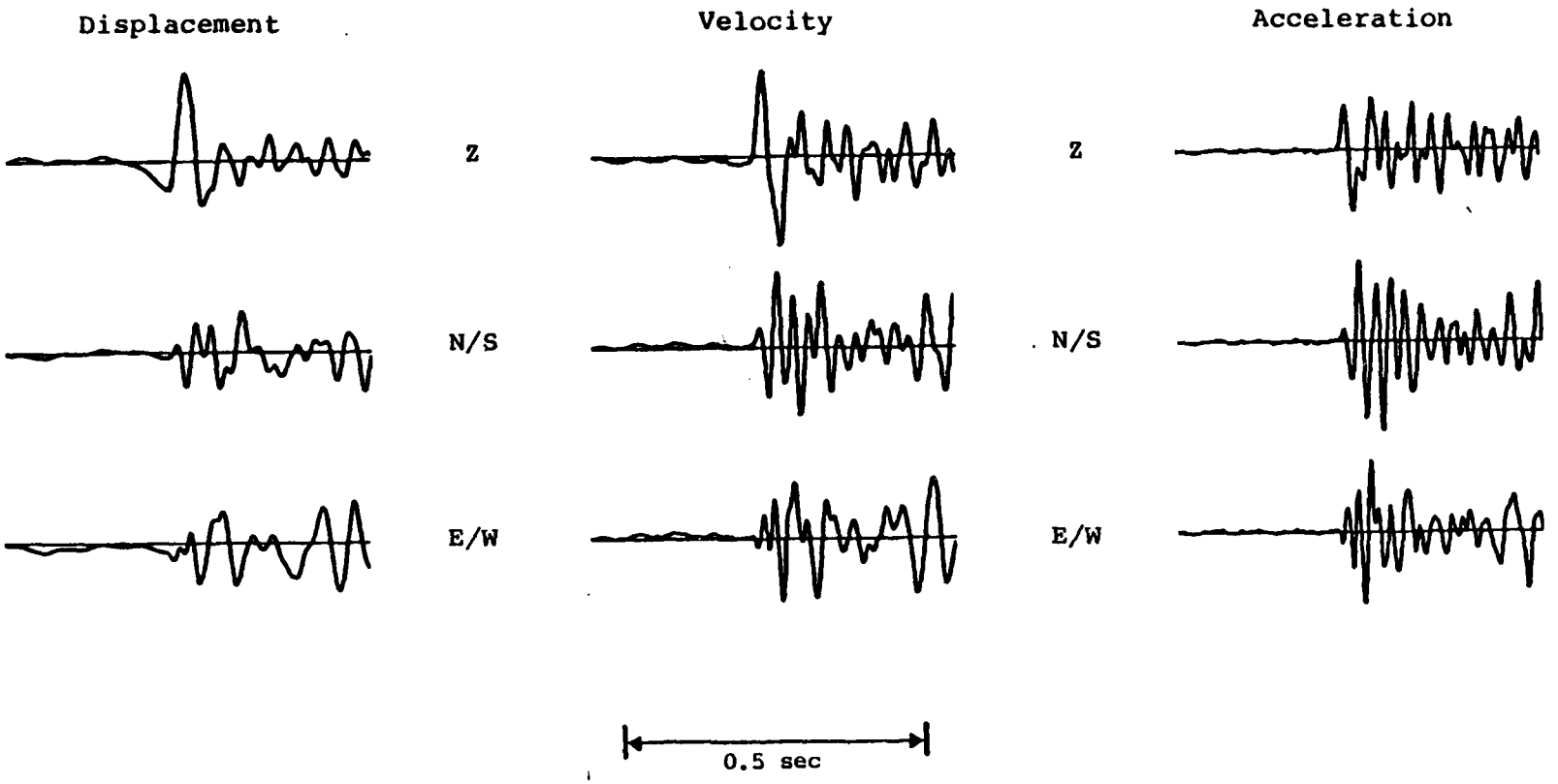

Figure 24. Comparison of vertical and horizontal components of displacement, velocity and acceleration recorded at ground zero from MILL YARD.

vector character of the motion can be examined. Now, in a plane-layered medium the initial P wave motion at ground zero would be expected to be negligible on the horizontal components, and it can be seen that this is essentially true for the displacement time-histories. However, in the progression to the higher frequency velocity and acceleration traces, this approximation begins to break down until, for the acceleration motion, the initial peak actually occurs on one of the horizontal components. This is rather surprising given the relatively uncomplicated vertical section through this propagation path shown previously in Figure 17 and provides further illustration of some of the complications which can obscure the interpretation of high frequency seismic data for identification purposes.

V. SUMMARY AND CONCLUSIONS

5.1 SUMMARY

Recently, Evernden et al. (1986) and others have suggested that the detection and identification of cavity decoupled nuclear explosions can best be carried out by seismic monitoring at frequencies above 20 Hz. However, this hypothesis is based, at least in part, upon the predictions of a highly oversimplified analytic seismic source model for decoupled explosions, and the applicability of this model at high frequencies has yet to be demonstrated either theoretically or experimentally. The investigations summarized in this interim report have centered on more rigorous investigations of the high frequency characteristics of such decoupled seismic sources. More specifically, a combination of detailed deterministic simulations and analyses of empirical data recorded from selected cavity decoupled explosions has been employed to investigate this issue.

A brief review of decoupling phenomenology was presented in Section II where the various decoupling criteria were defined and used to illustrate the dependence of the required cavity size on explosion yield and depth of burial. In addition, the classical step function pressure approximation to the decoupled seismic source function was compared with the seismic source corresponding to the more complex cavity pressure history predicted using nonlinear finite difference calculations in order to illustrate the discrepancies between these two source approximations at high frequencies.

The results of a series of detailed, nonlinear finite difference simulations of the seismic source functions corresponding to cavity decoupled explosions in unsaturated tuff and salt emplacement media were described in Section III where they were compared with the results of corresponding linear simulations. These comparisons were then used to

identify the mechanisms by which the initial transient pressure spike on the cavity wall induces nonlinear responses in these two media. As a result of this analysis, it was demonstrated that the use of a more realistic cavity pressure loading leads to significantly enhanced estimates of the seismic coupling at high frequency relative to that predicted by the simple step pressure approximation.

Preliminary analyses of high frequency seismic data recorded from the STERLING decoupled explosion in salt and the MILL YARD decoupled explosion in unsaturated tuff were presented in Section IV where an attempt was made to determine whether the theoretically predicted high frequency decoupling effects described in Section III could be detected in the observed seismic data. Using the results of these analyses, it was demonstrated that, while the high frequency source components associated with the complex cavity pressure loading do effectively couple into the seismic regime, the effects of propagation make it difficult to reliably extract these features from the measured data.

5.2 CONCLUSIONS

The results of the analyses described above support the following preliminary conclusions concerning the high frequency seismic source characteristics of cavity decoupled underground nuclear explosions.

(1) The results of a series of preliminary nonlinear finite difference simulations of cavity decoupling in tuff and salt emplacement media have confirmed that the simple step pressure approximation does not provide an adequate description of the high frequency seismic characteristics of such sources. In particular, all the simulations conducted to date indicate enhanced seismic coupling at high frequency relative to that predicted using the classical step pressure approximation.

(2) The nonlinear simulations also indicate that, while the Latter decoupling criterion may be approximately correct for salt, it is not adequate to prevent significant pressure-spike induced nonlinearities in unsaturated tuff. For both tuff and salt, however, the decoupling effectiveness obtained using the Patterson criterion is not significantly different from that obtained using the more conservative Latter criterion.

(3) The nature of the nonlinear response in unsaturated tuff is such that the decoupling effectiveness at low frequency is actually increased over that predicted by the linear, elastic solution. This reflects the fact that the predominant nonlinear mechanism in this medium is crush-up of the air filled porosity. In salt, on the other hand, where the predominant nonlinear mechanism is yielding, the nonlinear solution predicts decreased decoupling effectiveness relative to the linear, in accord with traditional decoupling concepts.

(4) Examination of the free-field data recorded from both the STERLING and MILL YARD nuclear decoupling experiments indicates that the high frequency source components associated with the actual complex cavity pressure loadings do effectively couple into the seismic regime, in agreement with the predictions of the nonlinear finite difference simulations.

(5) However, the observed complexity of the propagation effects at high frequency, as evidenced by the MILL YARD ground zero data, raises questions as to whether such source characteristics can be reliably recovered from the recorded seismic data and used for identification purposes.

REFERENCES

Brode, H. L. (1968), "Review of Nuclear Weapons Effects," Annual Review of Nuclear Science, 18, p. 153.

Evernden, J. F. (1976), "Study of Seismological Evasion Part I. General Discussion of Various Evasion Schemes," Bull. Seism. Soc. Am., 66, p. 245.

Evernden, J. F., C. Archambeau, E. Cranswick (1986), "An Evaluation of Seismic Decoupling and Underground Nuclear Test Monitoring Using High Frequency Seismic Data," Reviews of Geophysics, 24, pp. 143-215.

Garbin, H. D. (1986), "Free-Field and Decoupling Analysis of MILL YARD Data," Sandia Report SAND86-1702, December.

Heard, H. C., A. E. Abey, B. P. Bonner and A. Duba (1975), "Stress-Strain Behavior of Polycrystalline NACL to 3.2 GPa," Lawrence Livermore Laboratory Report, UCRL-51743.

Latter, A. L. (1959), "Verbatim Record of Technical Working Group 2, Conference on the Discontinuance of Nuclear Weapons Tests," GEN/DNT/TWG. 2/PV, December 2, 1959.

Latter, A. L., R. E. Lelevier, E. A. Martinelli and W. G. McMillan (1961), "A Method of Concealing Underground Nuclear Explosions," J. Geophys. Res., 66, p. 2929.

Mueller, R. A. and J. R. Murphy (1971), "Seismic Characteristics of Underground Nuclear Detonations," Bull. Seism. Soc. Am., 61, p. 1675.

Murphy, J. R. (1979), Proceedings of the ARPA Decoupling Conference," December.

Patterson, D. W. (1964), "Theory of Nuclear Explosion in a Cavity Including the Effects of Shock and Nonelastic Effects on the Wall and Comparison with Tamped Explosions - Project Dribble," UCRL-7916.

Rodean, H. C. (1971), "Cavity Decoupling of Nuclear Explosions," UCRL-51097.

Sisemore, C. J., L. A. Rogers and W. R. Perret (1969), "Project Sterling: Subsurface Phenomenology Measurements Near a Decoupled Nuclear Event," J. Geophys. Res., 74, p. 6623.

CONTRACTORS (United States)

Professor Keiiti Aki
Center for Earth Sciences
University of Southern California
University Park
Los Angeles, CA 90089-0741

Professor Charles B. Archambeau
Cooperative Institute for Resch
in Environmental Sciences
University of Colorado
Boulder, CO 80309

Dr. Thomas C. Bache Jr.
Science Applications Int'l Corp.
10210 Campus Point Drive
San Diego, CA 92121 (2 copies)

Dr. Douglas R. Baumgardt
Signal Analysis & Systems Div.
ENSCO, Inc.
5400 Port Royal Road
Springfield, VA 22151-2388

Dr. S. Bratt
Science Applications Int'l Corp.
10210 Campus Point Drive
San Diego, CA 92121

Dr. Lawrence J. Burdick
Woodward-Clyde Consultants
P.O. Box 93245
Pasadena, CA 91109-3245 (2 copies)

Professor Robert W. Clayton
Seismological Laboratory/Div. of
Geological & Planetary Sciences
California Institute of Technology
Pasadena, CA 91125

Dr. Vernon F. Cormier
Department of Geology & Geophysics
U-45, Roon 207
The University of Conneticut
Storrs, Connecticut 06268

Dr. Zoltan A. Der
ENSCO, Inc.
5400 Port Royal Road
Springfield, VA 22151-2388

Professor John Ferguson
Center for Lithospheric Studies
The University of Texas at Dallas
P.O. Box 830688
Richardson, TX 75083-0688

Professor Stanley Flatte'
Applied Sciences Building
University of California, Santa Cruz
Santa Cruz, CA 95064

Professor Steven Grand
Department of Geology
245 Natural History Building
1301 West Green Street
Urbana, IL 61801

Professor Roy Greenfield
Geosciences Department
403 Deike Building
The Pennsylvania State University
University Park, PA 16802

Professor David G. Harkrider
Seismological Laboratory
Div of Geological & Planetary Sciences
California Institute of Technology
Pasadena, CA 91125

Professor Donald V. Helmberger
Seismological Laboratory
Div of Geological & Planetary Sciences
California Institute of Technology
Pasadena, CA 91125

Professor Eugene Herrin
Institute for the Study of Earth
& Man/Geophysical Laboratory
Southern Methodist University
Dallas, TX 75275

Professor Robert B. Herrmann
Department of Earth & Atmospheric
Sciences
Saint Louis University
Saint Louis, MO 63156

Professor Lane R. Johnson
Seismographic Station
University of California
Berkeley, CA 94720

Professor Thomas H. Jordan
Department of Earth, Atmospheric
and Planetary Sciences
Mass Institute of Technology
Cambridge, MA 02139

Dr. Alan Kafka
Department of Geology &
Geophysics
Boston College
Chestnut Hill, MA 02167

Professor Leon Knopoff
University of California
Institute of Geophysics
& Planetary Physics
Los Angeles, CA 90024

Professor Charles A. Langston
Geosciences Department
403 Deike Building
The Pennsylvania State University
University Park, PA 16802

Professor Thorne Lay
Department of Geological Sciences
1006 C.C. Little Building
University of Michigan
Ann Harbor, MI 48109-1063

Dr. Randolph Martin III
New England Research, Inc.
P.O. Box 857
Norwich, VT 05055

Dr. Gary McCartor
Mission Research Corp.
735 State Street
P.O. Drawer 719
Santa Barbara, CA 93102 (2 copies)

Professor Thomas V. McEvilly
Seismographic Station
University of California
Berkeley, CA 94720

Dr. Keith L. McLaughlin
S-CUBED,
A Division of Maxwell Laboratory
P.O. Box 1620
La Jolla, CA 92038-1620

Professor William Menke
Lamont-Doherty Geological Observatory
of Columbia University
Palisades, NY 10964

Professor Brian J. Mitchell
Department of Earth & Atmospheric
Sciences
Saint Louis University
Saint Louis, MO 63156

Mr. Jack Murphy
S-CUBED
A Division of Maxwell Laboratory
11800 Sunrise Valley Drive
Suite 1212
Reston, VA 22091 (2 copies)

Professor J. A. Orcutt
Institute of Geophysics and Planetary
Physics, A-205
Scripps Institute of Oceanography
Univ. of California, San Diego
La Jolla, CA 92093

Professor Keith Priestley
University of Nevada
Mackay School of Mines
Reno, NV 89557

Wilmer Rivers
Teledyne Geotech
314 Montgomery Street
Alexandria, VA 22314

Professor Charles G. Sammis
Center for Earth Sciences
University of Southern California
University Park
Los Angeles, CA 90089-0741

Dr. Jeffrey L. Stevens
S-CUBED,
A Division of Maxwell Laboratory
P.O. Box 1620
La Jolla, CA 92038-1620

Professor Brian Stump
Institute for the Study of Earth & Man
Geophysical Laboratory
Southern Methodist University
Dallas, TX 75275

Professor Ta-liang Teng
Center for Earth Sciences
University of Southern California
University Park
Los Angeles, CA 90089-0741

Professor M. Nafi Toksoz
Earth Resources Lab
Dept of Earth, Atmospheric and
Planetary Sciences
Massachusetts Institute of Technology
42 Carleton Street
Cambridge, MA 02142

Professor Terry C. Wallace
Department of Geosciences
Building #11
University of Arizona
Tucson, AZ 85721

Weidlinger Associates
ATTN: Dr. Gregory Wojcik
620 Hansen Way, Suite 100
Palo Alto, CA 94304

Professor Francis T. Wu
Department of Geological Sciences
State University of new York
At Binghamton
Vestal, NY 13901

OTHERS (United States)

Dr. Monem Abdel-Gawad
Rockwell Internat'l Science Center
1049 Camino Dos Rios
Thousand Oaks, CA 91360

Professor Shelton S. Alexander
Geosciences Department
403 Deike Building
The Pennsylvania State University
University Park, PA 16802

Dr. Ralph Archuleta
Department of Geological
Sciences
Univ. of California at
Santa Barbara
Santa Barbara, CA

Dr. Muawia Barazangi
Geological Sciences
Cornell University
Ithaca, NY 14853

J. Barker
Department of Geological Sciences
State University of New York
at Binghamton
Vestal, NY 13901

Mr. William J. Best
907 Westwood Drive
Vienna, VA 22180

Dr. N. Biswas
Geophysical Institute
University of Alaska
Fairbanks, AK 99701

Dr. G. A. Bollinger
Department of Geological Sciences
Virginia Polytechnical Institute
21044 Derring Hall
Blacksburg, VA 24061

Dr. James Bulau
Rockwell Int'l Science Center
1049 Camino Dos Rios
P.O. Box 1085
Thousand Oaks, CA 91360

Mr. Roy Burger
1221 Serry Rd.
Schenectady, NY 12309

Dr. Robert Burridge
Schlumberger-Doll Resch Ctr.
Old Quarry Road
Ridgefield, CT 06877

Science Horizons, Inc.
ATTN: Dr. Theodore Cherry
710 Encinitas Blvd., Suite 101
Encinitas, CA 92024 (2 copies)

Professor Jon F. Claerbout
Professor Amos Nur
Dept. of Geophysics
Stanford University
Stanford, CA 94305 (2 copies)

Dr. Anton W. Dainty
AFGL/LWH
Hanscom AFB, MA 01731

Dr. Steven Day
Dept. of Geological Sciences
San Diego State U.
San Diego, CA 92182

Professor Adam Dziewonski
Hoffman Laboratory
Harvard University
20 Oxford St.
Cambridge, MA 02138

Professor John Ebel
Dept of Geology & Geophysics
Boston College
Chestnut Hill, MA 02167

Dr. Alexander Florence
SRI International
333 Ravenswood Avenue
Menlo Park, CA 94025-3493

Dr. Donald Forsyth
Dept. of Geological Sciences
Brown University
Providence, RI 02912

Dr. Anthony Gangi
Texas A&M University
Department of Geophysics
College Station, TX 77843

Dr. Freeman Gilbert
Institute of Geophysics &
Planetary Physics
Univ. of California, San Diego
P.O. Box 109
La Jolla, CA 92037

Mr. Edward Giller
Pacific Seirra Research Corp.
1401 Wilson Boulevard
Arlington, VA 22209

Dr. Jeffrey W. Given
Sierra Geophysics
11255 Kirkland Way
Kirkland, WA 98033

Dr. Henry L. Gray
Associate Dean of Dedman College
Department of Statistical Sciences
Southern Methodist University
Dallas, TX 75275

Rong Song Jih
Teledyne Geotech
314 Montgomery Street
Alexandria, Virginia 22314

Professor F.K. Lamb
University of Illinois at
Urbana-Champaign
Department of Physics
1110 West Green Street
Urbana, IL 61801

Dr. Arthur Lerner-Lam
Lamont-Doherty Geological Observatory
of Columbia University
Palisades, NY 10964

Dr. L. Timothy Long
School of Geophysical Sciences
Georgia Institute of Technology
Atlanta, GA 30332

Dr. Peter Malin
University of California at Santa Barbara
Institute for Central Studies
Santa Barbara, CA 93106

Dr. George R. Mellman
Sierra Geophysics
11255 Kirkland Way
Kirkland, WA 98033

Dr. Bernard Minster
Institute of Geophysics and Planetary
Physics, A-205
Scripps Institute of Oceanography
Univ. of California, San Diego
La Jolla, CA 92093

Professor John Nabelek
College of Oceanography
Oregon State University
Corvallis, OR 97331

Dr. Geza Nagy
U. California, San Diego
Dept of Ames, M.S. B-010
La Jolla, CA 92093

Dr. Jack Oliver
Department of Geology
Cornell University
Ithaca, NY 14850

Dr. Robert Phinney/Dr. F.A. Dahlen
Dept of Geological
Geophysical Sci. University
Princeton University
Princeton, NJ 08540 (2 copies)

RADIX Systems, Inc.
Attn: Dr. Jay Pulli
2 Taft Court, Suite 203
Rockville, Maryland 20850

Professor Paul G. Richards
Lamont-Doherty Geological
Observatory of Columbia Univ.
Palisades, NY 10964

Dr. Norton Rimer
S-CUBED
A Division of Maxwell Laboratory
P.O. 1620
La Jolla, CA 92038-1620

Professor Larry J. Ruff
Department of Geological Sciences
1006 C.C. Little Building
University of Michigan
Ann Arbor, MI 48109-1063

Dr. Alan S. Ryall, Jr.
Center of Seismic Studies
1300 North 17th Street
Suite 1450
Arlington, VA 22209-2308 (4 copies)

Dr. Richard Sailor
TASC Inc.
55 Walkers Brook Drive
Reading, MA 01867

Thomas J. Sereno, Jr.
Service Application Int'l Corp.
10210 Campus Point Drive
San Diego, CA 92121

Dr. David G. Simpson
Lamont-Doherty Geological Observ.
of Columbia University
Palisades, NY 10964

Dr. Bob Smith
Department of Geophysics
University of Utah
1400 East 2nd South
Salt Lake City, UT 84112

Dr. S. W. Smith
Geophysics Program
University of Washington
Seattle, WA 98195

Dr. Stewart Smith
IRIS Inc.
1616 N. Fort Myer Drive
Suite 1440
Arlington, VA 22209

Rondout Associates
ATTN: Dr. George Sutton,
Dr. Jerry Carter, Dr. Paul Pomeroy
P.O. Box 224
Stone Ridge, NY 12484 (4 copies)

Dr. L. Sykes
Lamont Doherty Geological Observ.
Columbia University
Palisades, NY 10964

Dr. Pradeep Talwani
Department of Geological Sciences
University of South Carolina
Columbia, SC 29208

Dr. R. B. Tittmann
Rockwell International Science Center
1049 Camino Dos Rios
P.O. Box 1085
Thousand Oaks, CA 91360

Professor John H. Woodhouse
Hoffman Laboratory
Harvard University
20 Oxford St.
Cambridge, MA 02138

Dr. Gregory B. Young
ENSCO, Inc.
5400 Port Royal Road
Springfield, VA 22151-2388

OTHERS (FOREIGN)

Dr. Peter Basham
Earth Physics Branch
Geological Survey of Canada
1 Observatory Crescent
Ottawa, Ontario
CANADA K1A 0Y3

Dr. Eduard Berg
Institute of Geophysics
University of Hawaii
Honolulu, HI 96822

Dr. Michel Bouchon - Universite
Scientifique et Medicale de Grenob
Lab de Geophysique - Interne et
Tectonophysique - I.R.I.G.M-B.P.
38402 St. Martin D'Heres
Cedex FRANCE

Dr. Hilmar Bungum/NTNF/NORSAR
P.O. Box 51
Norwegian Council of Science,
Industry and Research, NORSAR
N-2007 Kjeller, NORWAY

Dr. Michel Campillo
I.R.I.G.M.-B.P. 68
38402 St. Martin D'Heres
Cedex, FRANCE

Dr. Kin-Yip Chun
Geophysics Division
Physics Department
University of Toronto
Ontario, CANADA M5S 1A7

Dr. Alan Douglas
Ministry of Defense
Blacknest, Brimpton,
Reading RG7-4RS
UNITED KINGDOM

Dr. Manfred Henger
Fed. Inst. For Geosciences & Nat'l Res.
Postfach 510153
D-3000 Hannover 51
FEDERAL REPUBLIC OF GERMANY

Dr. E. Husebye
NTNF/NORSAR
P.O. Box 51
N-2007 Kjeller, NORWAY

Ms. Eva Johannisson
Senior Research Officer
National Defense Research Inst.
P.O. Box 27322
S-102 54 Stockholm
SWEDEN

Tormod Kvaerna
NTNF/NORSAR
P.O. Box 51
N-2007 Kjeller, NORWAY

Mr. Peter Marshall, Procurement
Executive, Ministry of Defense
Blacknest, Brimpton,
Reading FG7-4RS
UNITED KINGDOM (3 copies)

Dr. Ben Menaheim
Weizman Institute of Science
Rehovot, ISRAEL 951729

Dr. Svein Mykkeltveit
NTNF/NORSAR
P.O. Box 51
N-2007 Kjeller, NORWAY (3 copies)

Dr. Robert North
Geophysics Division
Geological Survey of Canada
1 Observatory crescent
Ottawa, Ontario
CANADA, K1A OY3

Dr. Frode Ringdal
NTNF/NORSAR
P.O. Box 51
N-2007 Kjeller, NORWAY

Dr. Jorg Schlittenhardt
Federal Inst. for Geosciences & Nat'l Res.
Postfach 510153
D-3000 Hannover 51
FEDERAL REPUBLIC OF GERMANY

University of Hawaii
Institute of Geophysics
ATTN: Dr. Daniel Walker
Honolulu, HI 96822

FOREIGN CONTRACTORS

Dr. Ramon Cabre, S.J.
c/o Mr. Ralph Buck
Economic Consular
American Embassy
APO Miami, Florida 34032

Professor Peter Harjes
Institute for Geophysik
Rhur University/Bochum
P.O. Box 102148 4630 Bochum 1
FEDERAL REPUBLIC OF GERMANY

Professor Brian L.N. Kennett
Research School of Earth Sciences
Institute of Advanced Studies
G.P.O. Box 4
Canberra 2601
AUSTRALIA

Dr. B. Massinon
Societe Radiomana
27, Rue Claude Bernard
7,005, Paris, FRANCE (2 copies)

Dr. Pierre Mechler
Societe Radiomana
27, Rue Claude Bernard
75005 Paris, FRANCE

GOVERNMENT

Dr. Ralph Alewine III
DARPA/NMRO
1400 Wilson Boulevard
Arlington, VA 22209-2308

Dr. Peter Basham
Geological Survey of Canada
1 Observatory Creseut
Ottowa, Ontario
CANADA K1A OY3

Dr. Robert Blandford
DARPA/NMRO
1400 Wilson Boulevard
Arlington, VA 22209-2308

Sandia National Laboratory
ATTN: Dr. H. B. Durham
Albuquerque, NM 87185

Dr. Jack Evernden
USGS-Earthquake Studies
345 Middlefield Road
Menlo Park, CA 94025

U.S. Geological Survey
ATTN. Dr. T. Hanks
Nat'l Earthquake Resch Center
345 Middlefield Road
Menlo Park, CA 94025

Dr. James Hannon
Lawrence Livermore Nat'l Lab.
P.O. Box 808
Livermore, CA 94550

U.S. Arms Control & Disarm. Agency
ATTN: Dick Morrow
Washington, D.C. 20451

Paul Johnson
ESS-4, Mail Stop J979
Los Alamos National Laboratory
Los Alamos, NM 87545

Ms. Ann Kerr
DARPA/NMRO
1400 Wilson Boulevard
Arlington, VA 22209-2308

Dr. Max Koontz
US Dept of Energy/DP 331
Forrestal Building
1000 Independence Ave.
Washington, D.C. 20585

Dr. W. H. K. Lee
USGS
Office of Earthquakes, Volcanoes,
& Engineering
Branch of Seismology
345 Middlefield Rd
Menlo Park, CA 94025

Dr. William Leith
USGS
Mail Stop 928
Reston, VA 22092

Dr. Richard Lewis
Dir. Earthquake Engineering and
Geophysics
U.S. Army Corps of Engineers
Box 631
Vicksburg, MS 39180

Dr. Robert Masse'
Box 25046, Mail Stop 967
Denver Federal Center
Denver, Colorado 80225

R. Morrow
ACDA/VI
Room 5741
320 21st Street N.W.
Washington, D.C. 20451

Dr. Keith K. Nakanishi
Lawrence Livermore National Laboratory
P.O. Box 808, L-205
Livermore, CA 94550 (2 copies)

Dr. Carl Newton
Los Alamos National Lab.
P.O. Box 1663
Mail Stop C335, Group E553
Los Alamos, NM 87545

Dr. Kenneth H. Olsen
Los Alamos Scientific Lab.
Post Office Box 1663
Los Alamos, NM 87545

Howard J. Patton
Lawrence Livermore National Laboratory
P.O. Box 808, L-205
Livermore, CA 94550

Mr. Chris Paine
Office of Senator Kennedy
SR 315
United States Senate
Washington, D.C. 20510

AFOSR/NP
ATTN: Colonel Jerry J. Perrizo
Bldg 410
Bolling AFB, Wash D.C. 20332-6448

HQ AFTAC/TT
Attn: Dr. Frank F. Pilotte
Patrick AFB, Florida 32925-6001

Mr. Jack Rachlin
USGS - Geology, Rm 3 C136
Mail Stop 928 National Center
Reston, VA 22092

Robert Reinke
AFWL/NTESG
Kirtland AFB, NM 87117-6008

HQ AFTAC/TGR
Attn: Dr. George H. Rothe
Patrick AFB, Florida 32925-6001

Donald L. Springer
Lawrence Livermore National Laboratory
P.O. Box 808, L-205
Livermore, CA 94550

Dr. Lawrence Turnbull
OSWR/NED
Central Intelligence Agency
CIA, Room 5G48
Washington, D.C. 20505

Dr. Thomas Weaver
Los Alamos Scientific Laboratory
Los Almos, NM 97544

AFGL/SULL
Research Library
Hanscom AFB, MA 01731-5000 (2 copies)

Secretary of the Air Force (SAFRD)
Washington, DC 20330
Office of the Secretary Defense
DDR & E
Washington, DC 20330

HQ DNA
ATTN: Technical Library
Washington, DC 20305

Director, Technical Information
DARPA
1400 Wilson Blvd.
Arlington, VA 22209

AFGL/XO
Hanscom AFB, MA 01731-5000

AFGL/LW
Hanscom AFB, MA 01731-5000

DARPA/PM
1400 Wilson Boulevard
Arlington, VA 22209

Defense Technical
Information Center
Cameron Station
Alexandria, VA 22314
(5 copies)

Defense Intelligence Agency
Directorate for Scientific &
Technical Intelligence
Washington, D.C. 20301

Defense Nuclear Agency/SPSS
ATTN: Dr. Michael Shore
6801 Telegraph Road
Alexandria, VA 22310

AFTAC/CA (STINFO)
Patrick AFB, FL 32925-6001

Dr. Gregory van der Vink
Congress of the United States
Office of Technology Assessment
Washington, D.C. 20510